Pacific Northwest NATIONAL LABORATORY

PNNL-27419

April 2018

J Matyáš
GJ Sevigny
JJ Venarsky
JM Davis
CD Lukins
JB Lang
MK Edwards
CM Stewart
SE Sannoh
TG Veldman
NR Phillips
CM Fischer

Prepared for the U.S. Department of Energy under **Contract DE-AC05-76RL01830**

U.S. DEPARTMENT OF ENERGY

DISCLAIMER

PACIFIC NORTHWEST NATIONAL LABORATORY
operated by
BATTELLE
for the
UNITED STATES DEPARTMENT OF ENERGY
under Contract DE-AC05-76RL01830

Printed in the United States of America

Available to DOE and DOE contractors from the
Office of Scientific and Technical Information,
P.O. Box 62, Oak Ridge, TN 37831-0062;
ph: (865) 576-8401
fax: (865) 576-5728
email: reports@adonis.osti.gov

Available to the public from the National Technical Information Service
5301 Shawnee Rd., Alexandria, VA 22312
ph: (800) 553-NTIS (6847)
email: orders@ntis.gov <http://www.ntis.gov/about/form.aspx>
Online ordering: http://www.ntis.gov

PNNL-27419
EWG-RPT-018

Evaluation of Crystal Accumulation in High-Level Waste Glasses with Research-Scale Melter

April 2018

J Matyáš
GJ Sevigny
JJ Venarsky
JM Davis
CD Lukins
JB Lang
MK Edwards
CM Stewart
SE Sannoh
TG Veldman
NR Phillips
CM Fischer

Prepared for
the U.S. Department of Energy
under Contract DE-AC05-76RL01830

Pacific Northwest National Laboratory
Richland, Washington 99352

Executive Summary

This report presents in detail experimental results from a long-term research-scale melter (RSM) test that was performed at Pacific Northwest National Laboratory in FY 2016 to answer questions on the effects of spinel crystal accumulation on melter performance and operational longevity. The RSM was used to vitrify a surrogate-waste material of the Hanford AZ-101 tank waste composition. This waste contains a high concentration of Fe and Ni and is susceptible to precipitation of a large quantity of spinel crystals during vitrification. The RSM test was run over a period of 11 weeks and consisted of 11 feeding/pouring and idling periods. The feeding/pouring periods were 36 h long, while the idling periods ranged from 4 to 7 days. Approximately 509 kg of feed were processed, producing ~159 kg of glass. The main goal of this test was to determine whether the riser of the melter can be clogged by an accumulated layer of spinel crystals that precipitated from glass during multiple idling periods. In addition, glass samples were collected during each pouring to evaluate the possibility of a partial or complete removal of crystal deposits that had accumulated during idling. Furthermore, an electrical conductivity probe was tested for monitoring the crystal accumulation in the riser of the melter during idlings. The test was concluded by dissecting the melter and preparing cross sections to determine layer thickness, crystal size, and morphology of spinel crystals in the bulk of the melter and in the glass-discharge riser.

Two overfeeding incidents, caused by a faulty latch on a peristaltic pump, that occurred during the seventh feeding/pouring period resulted in an increased temperature of poured glass and vigorous discharge of molten glass. These conditions led to removal of layers of spinel accumulated over seven idling periods. In spite of that, a significant accumulation of spinel crystals occurred in the bulk of the melter and in the 30° sloped and vertical sections of the riser during the following four idling periods. In the bulk of the melter, the thickness of the accumulated layer varied from 0.5 to 3.4 cm. Thicker deposits formed towards the wall of the melter due to currents induced by the bubbler and natural convection from temperature differences in the molten glass. In the glass-discharge riser section, a ~1.4 cm thick crystal bank formed at the entry point of the 30° sloped section, obstructing more than 60% of the opening (2.3 cm). After that, the layer thickness decreased to 1.2 cm and was nearly constant throughout. In the vertical section of the riser, the dead flow zone in the corner together with crystal accumulation resulted in a layer that obstructed about half of the opening.

Crystal accumulation in the same glass was also studied in the laboratory using a previously developed double-crucible approach. The crystal accumulation rate, 0.653 mm/day, was about two times higher than the one observed in the RSM test. The lower accumulation rate for the RSM test can be justified by 1) small-scale removal of the layer during pouring, 2) nonuniform temperature distribution in the riser, which sets up temperature-gradient convection that disrupts density-difference–driven settling of crystals, and 3) small crystals already present in the RSM glass before idling began (these crystals act as nucleation sites, which would result in a high concentration of small crystals that settle slowly or, if smaller than 10 μm, remain suspended in the glass). The crystals obtained from the double-crucible test were about 40% bigger (~72–74 μm) than crystals observed for the RSM test (~44 μm). Crystal fraction in accumulated layers was about the same for double-crucible (23.8–25.4%) and RSM tests (24.4%).

X-ray diffraction analysis of glass samples collected after different time intervals during glass pouring showed a large variation of crystal concentrations in the glass: from 0.2 to 3.9 mass%. At peaks, the concentrations were significantly higher than concentrations of crystals in the bulk

of the melter, which varied from 0.3 to 1.1 mass%. This suggests that the accumulated layer may be disturbed and a small fraction removed during regular pouring events.

Electrical conductivity probe testing showed that this method can be used to monitor accumulation of spinel crystals in the riser section of the melter. However, more tests are needed to develop this method to the stage of commercial use. Electrical conductivity data collected over the period of four idlings showed a layer growth rate of ~0.346 mm/day. Extrapolating this rate for a total idling time of 66 days during this test and estimating that the layer was not disturbed by pouring indicates that a layer 22.8 mm thick can accumulate over that time. This layer would almost completely (99.5%) clog the riser opening (23 mm).

The long-term RSM test also showed that more attention should be paid to the off-gas system. Maintenance was required on a regular basis to prevent clogging of the off-gas system.

Acknowledgments

Authors gratefully acknowledge the financial support of the U.S. Department of Energy (DOE) Office of River Protection Waste Treatment and Immobilization Plant Project as managed by Albert A. Kruger. The authors also thank Mike Schweiger for a careful review and for all the comments/suggestions and Maura Zimmerschied for editorial assistance. Pacific Northwest National Laboratory is operated for the DOE by Battelle Memorial Institute under Contract DE-AC05-76RL01830.

Acronyms and Abbreviations

cfm	cubic feet per minute
DAC	data acquisition and control
DOE	U.S. Department of Energy
EVS	ejector venturi scrubber
HEME	high-efficiency mist elimination
HLW	high-level waste
PDL-E	Process Development Laboratory-East
PNNL	Pacific Northwest National Laboratory
RSM	research-scale melter
SEM	scanning electron microscope
slpm	standard liter(s) per minute
WG	water gauge
WTP	Hanford Tank Waste Treatment and Immobilization Plant
XRD	x-ray diffraction

Contents

Figures

Tables

1.0 Introduction

Immobilization of the nation's high-level nuclear waste requires the design, construction, and operation of large and technically complex one-of-a-kind waste treatment processing and vitrification facilities. Vitrification technology was selected to treat the high-level waste (HLW) fraction of tank waste at the U.S. Department of Energy's (DOE's) Hanford and Savannah River Sites, the low-activity waste fraction of tank waste at Hanford, and the sodium-bearing tank waste or calcined HLW at Idaho National Laboratory. Joule-heated ceramic melters are being used at the Defense Waste Processing Facility and will be used at the Hanford Tank Waste Treatment and Immobilization Plant (WTP) to vitrify radioactive waste.

Research-scale melter (RSM) tests at Pacific Northwest National Laboratory (PNNL) are intended to provide programmatic guidance to the WTP mission for efficient vitrification of a variety of Hanford tank waste streams. The results described here were the product of a test performed in FY 2016. The test was part of the DOE Office of River Protection (DOE-ORP) melter validation tests at PNNL. A high-Fe-Ni glass, developed at PNNL for Hanford AZ-101 tank waste, was used to investigate the effect of spinel crystallization on the operation of the RSM.

Idling of HLW melters is anticipated during vitrification campaigns due to the complexity of the operation at WTP and the complex composition of Hanford tank waste streams, which is further complicated by constant change as chemical reactions and radioactive decay occur. During idling, the temperature of the melt pool is decreased from 1150 °C to 1050 °C to extend the life of refractory lining. However, a lower temperature encourages crystallization of spinel crystals in the melt pool and glass-discharge riser. These crystals do not decrease durability of glass, but if accumulated in thick layers they can clog the riser and prevent pouring of the molten glass into canisters. A previous RSM test with the same glass was conducted with three seven-day idling periods and resulted in a 6-mm-thick layer in the riser (Matyáš et al 2015). The test described here was similar, except the number of idlings increased to 11. The long-term RSM test was designed to determine whether the riser of the melter can be clogged by accumulated layers of spinel crystals over a larger number of idling periods. Also tested was an electrical conductivity probe to monitor crystal accumulation in the riser of the melter.

The RSM test was run over a period of 11 weeks and consisted of 11 feeding/pouring and idling periods. The feeding/pouring periods were 36 h long, while the idling periods ranged from 4 to 7 days depending upon staff scheduling and availability. Approximately 509 kg of feed was processed, producing ~159 kg of glass. The glass samples were collected during each pouring and were analyzed for concentration of spinel crystals with x-ray diffraction (XRD). This was done to evaluate the possibility of a partial or complete removal of crystal deposits accumulated during idling. The test was concluded by dissecting the melter and preparing cross sections to determine layer thickness, crystal size, and morphology of spinel crystals in the bulk of the melter and in the glass-discharge riser.

2.0 Objectives

An effort is being made to fully utilize joule-heated ceramic melters and increase the loading of Hanford tank wastes in glass while meeting glass property and composition constraints and melter lifetime expectancies. Of key interest is crystal accumulation in the glass-discharge riser of the melter during idling.

The RSM test had two primary objectives. The first objective was to show that multiple idlings of the melter may result in the riser of the melter being clogged by an accumulated layer of spinel crystals. The second objective was to demonstrate applicability of an electrical conductivity probe method developed for real-time monitoring of crystal accumulation in the riser. The other requirements of this study were 1) to obtain steady-state operations and determine processing rate and melter operating characteristics, 2) to complete three to four crucible volume turnovers for each feeding segment in an attempt to disturb the deposited layer of crystals, 3) to complete seven or more feeding/pouring and idling periods (ranging from 4 to 7 days) to attempt to clog the glass-discharge riser before the end of the test, 4) to determine the concentration of spinel in poured glass samples collected at different times during idlings, and 5) to prepare cross sections of the riser and bulk melter and determine the thickness of accumulated spinel crystal layers, crystal size, and concentration of spinel crystals. In addition, these data were to be compared with lab-scale data from double-crucible tests.

3.0 RSM System Description

The RSM processing system is located at the Process Development Laboratory-East (PDL-E). A schematic of this system is shown in Figure 3.1 with liquid lines shown in blue and gas lines in black.

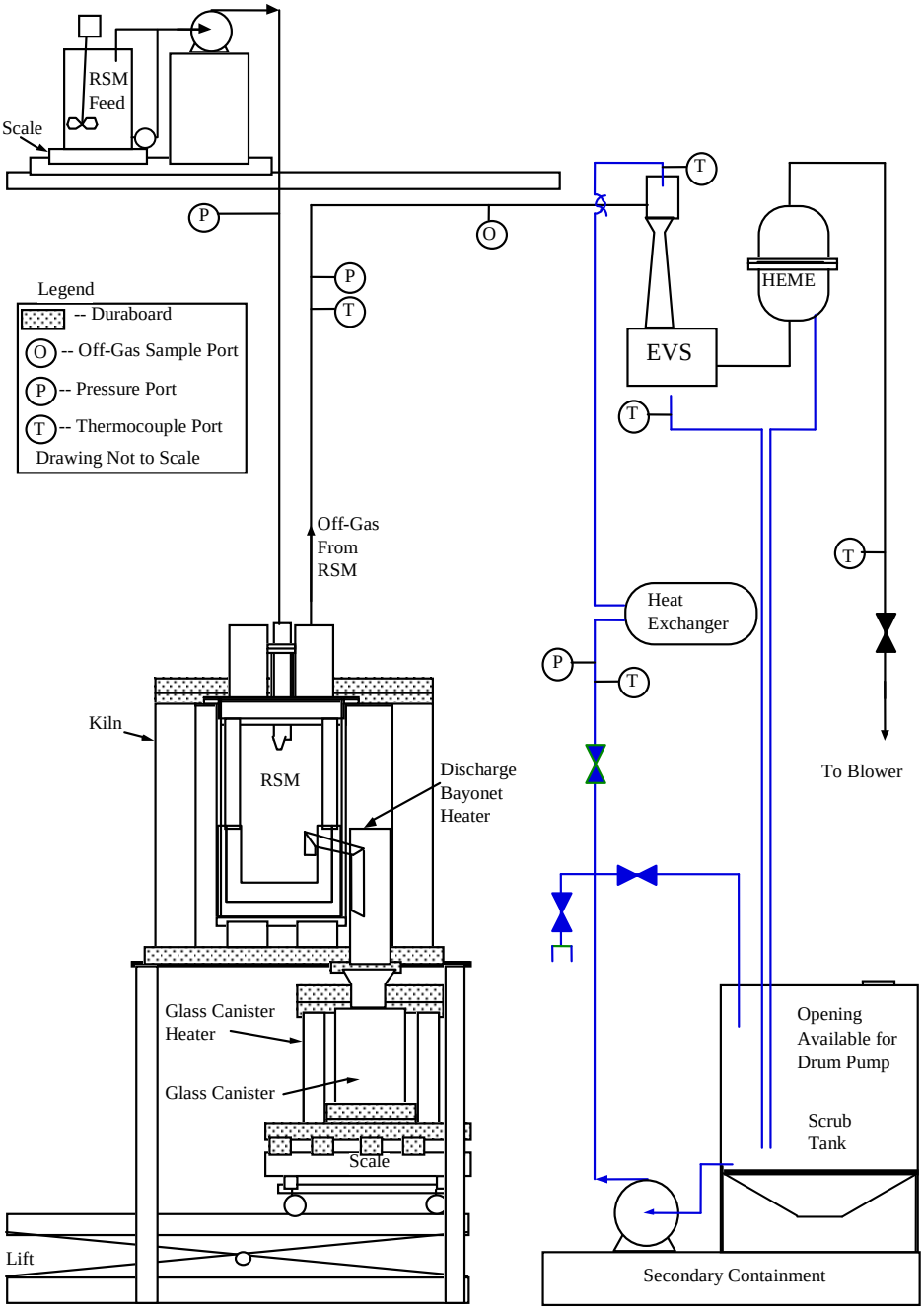

Figure 3.1. RSM Processing System

The RSM is designed to simulate processing of melter feed (feeding, melting, idling, and pouring) for a full-scale melter system. Its small scale allows for parametric studies that may be conducted in a relatively short time using a small amount of surrogate waste feed. Table 3.1 provides dimensions and operational characteristics of the RSM. Figure 3.2 illustrates its appearance. The RSM is made of an Inconel 625 closed-end cylinder that is lined with Alfrax® refractory, and contains a Monofrax® K-3 melting crucible with a glass-discharge riser and pour spout for discharge of the molten glass into a stainless steel canister. The melting crucible is 15.2 cm in diameter and 14.0 cm tall, and is equipped with a glass-discharge outlet 1.9 cm in diameter. The discharge outlet starts near the bottom of the crucible with a 30° slanted section, continues with a riser section approximately 7 cm tall (equipped with an electrical conductivity probe for monitoring of crystal accumulation), and is completed by a pour spout section before an overflow through a hole in the refractory.

An electric kiln surrounds the melter body for melting of 4 kg of previously melted and crushed high-Fe-Ni glass (used for melter start-up). A path through molten glass of sufficiently low resistance between electrodes is required to sustain Joule-effect heating. The kiln also minimizes heat loss during operation by decreasing the temperature gradient across the crucible wall. The glass-discharge section can be heated to 1100 °C using silicon carbide rod heaters to facilitate efficient pouring of the glass. A stainless steel canister is located below the pour spout and collects the glass. The canister can be heated if needed. However, this was avoided during this test. The focus was on the long-term performance of the melter and not on the behavior of the glass during cooling.

The joule heating is provided by two Inconel 693 electrodes, which enter the melter through ports in the lid and rest on the bottom of the crucible. Accounting for the areas covered by the electrodes and the bubbler, the melt surface area of the RSM is 172 cm^2. A nominal glass depth of 10.5 cm results in a glass inventory of 4.5 kg, assuming a glass density of 2.5 g/cm^3 at 1150 °C. The melter is controlled using a data acquisition and control (DAC) system, which regulates temperature, feed rate, bubbling rate, melter vacuum, and power supply to the melt crucible, pour spout heaters, and the surrounding kiln. Alarms on the DAC system are set to alert the operators if the melter control parameters drift outside of targeted ranges.

Table 3.1. RSM Dimensions and Operational Characteristics

Parameter	Characteristic
Melter cavity diameter	15.2 cm
Melt surface area[(a)]	172 cm^2
Melter cavity height	14.0 cm
Melter internal volume	2.55 L
Nominal glass melt depth	10.5 cm
Nominal glass melt volume	1.8 L
Maximum operating temperature	1200 °C
Nominal operating temperature for borosilicate glass	1150 °C
Bubbler dimensions	¼" OD tubing
Bubbler material	Inconel 690
Electrode plate dimensions (W × H × T)	11 × 10 × 0.9 cm
Electrode material	Inconel 693
Electrode distance from bottom	0 cm
Electrode current (average)	21.1 A
Electrode voltage (average)	101.5 V
Electrode current density (average)	0.19 A/cm^2

(a) Excluding areas covered by electrodes and bubblers

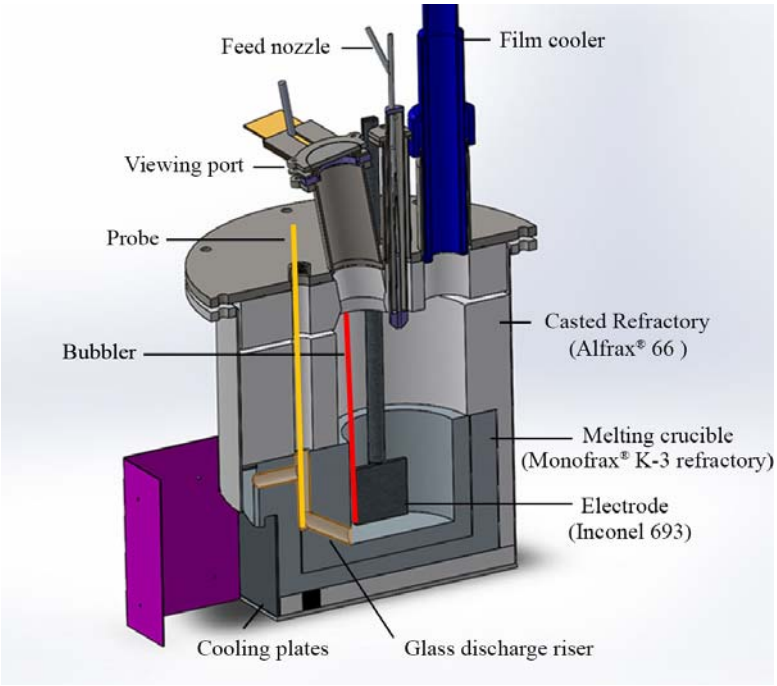

Figure 3.2. RSM Melter

The feed is delivered to the melter from the feed tank through a feed nozzle by a set of peristaltic pumps. The first pump recirculates the feed between the feed tank and a point near the melter to keep solids in the line suspended. The second pump draws feed from this recirculation line and controls the feed rate. An agitator in the feed tank keeps the feed well

mixed at all times. In addition, the feed tank is mounted on a scale, and its weight is monitored by the DAC system.

The RSM off-gas treatment is based on quenching of the hot off-gas, wet scrubbing, and high-efficiency mist elimination, as shown in Figure 3.1. The off-gas system contains a film cooler (Figure 3.2) fabricated from a sintered metal filter that allows injected air to pass from the outside of the filter through the sintered metal and into the off-gas line. This design allows exhaust gas to pass through the middle of the filter and combine with the injected air, resulting in the condensation of off-gas components. The aqueous quench scrubber is located downstream of the film cooler and is an ejector venturi scrubber (EVS) system previously shown to be functionally equivalent to the WTP submerged-bed scrubber technology (Goles and Schmidt 1992). The EVS system provides a constant mist of continuously recirculated EVS solution. Off-gas components that are not condensed by the film cooler are captured by the EVS mist and removed from the exhaust stream. The exhaust downstream of the EVS system is treated by a high-efficiency mist eliminator (HEME) that demists the influent stream and efficiently removes any submicron-size aerosol matter that penetrates the EVS system.

The EVS system sprays scrubber solution through a nozzle for direct contact with the melter exhaust. At the beginning of a melter run, the scrubber solution consists only of water. As the melter operates, the EVS system condenses water and particulates from the melter exhaust while also removing acidic gases. The resulting two-phase stream travels through a separator chamber and the scrubber solution returns to the scrub tank under the force of gravity. The scrubber solution is continuously recirculated within the EVS system. Downstream from the scrubber, the exhaust gases pass through a HEME to remove condensed-phase aerosols. HEME solution samples and EVS solution samples are collected periodically during each test and can be analyzed as needed.

4.0 Test Conditions

4.1 Summary

The RSM test was run over a period of 11 weeks and consisted of 11 feeding/pouring and idling periods. The feeding/pouring periods were ~36 h long with a target to obtain at least three melt volume turnovers per cycle, producing ~14.5 kg of glass. The melter operated with continuous feeding during each feeding/pouring period. Periodic sampling of the glass was performed during each feeding/pouring period to evaluate the concentration of spinel crystals in the glass. At the conclusion of each feeding/pouring period, the melter was idled from 4 to 7 days at 1050 °C. The periodic measurements of the accumulated spinel crystal layer were attempted using a conductivity probe installed in the riser section of the melter. Testing was terminated after processing of all feed and producing a total of ~159 kg of glass.

At the conclusion of the test, the melt pool was rapidly cooled by pumping water into the crucible to prevent additional crystallization. Then, the melter was dissected and the prepared cross sections were analyzed to determine layer thickness, crystal size, and composition of spinel crystals in the bulk of the melter and in the glass-discharge riser area.

4.2 Process Conditions

The overall process conditions maintained during each feeding/pouring period are described below, with targeted operating conditions listed in Table 4.1. The major parameters monitored throughout the duration of the test include the following:

1. Glass pool temperature

   The targeted glass pool temperature of 1150 °C was maintained and automatically controlled by the RSM's DAC system. The set point temperature of the kiln surrounding the melter was adjusted, if necessary, to maintain a stable glass temperature. Thermocouples were located next to each electrode and were used to monitor melt pool temperature.

2. Melter vacuum

   The melter vacuum was automatically controlled at a set point between 0.1 and 3.0 inches of water gauge (WG) below ambient atmospheric pressure, from 100.6 to 101.3 kPa. The RSM exhaust blower can provide up to 28 in. WG vacuum (at 200 cfm), most of which is dropped across the control valve under standard operating conditions. On-line differential pressures and percent valve opening parameters provided direct indications of development of off-gas line obstructions. A special tube of appropriate length was inserted through the sampling port on the off-gas elbow located downstream of the film cooler to remove any obstructions that developed in the film cooler during operation. Regularly scheduled cleaning of the film cooler was performed at the end of each feeding/pouring and idling period.

3. Bubbling rate

   Agitation of the molten glass pool using subsurface air injection was employed to enhance melter feed processing rates. A mass flow controller delivered air to the melt pool at 1.4 slpm via a single submerged Inconel 690 tube located near one of the electrodes. This bubbler flow rate was selected to maximize operational stability and to maintain system compatibility with other operational constraints.

Table 4.1. Targeted Operating Conditions

Parameter	Target
Melt surface area, cm^2	172
Melt volume, L	1.8
Glass density at room temperature, g/cm^3	2.5–2.65
Melter glass inventory, kg	4.5
Minimum expected glass rate, kg/h	0.3
Maximum expected glass rate, kg/h	0.8
Minimum expected feed rate, kg/h	1.3
Maximum expected feed rate, kg/h	2.6
Glass melt temperature, °C	1150
Plenum temperature range, °C	350–650
Plenum vacuum, inches of water gauge (WG) below atmospheric pressure	0.1–3.0
Post-film-cooler temperature range, °C	150–350
Bubbling rate, slpm	1.4
Initial scrub solution volume, L	80
Melter condensate, pH	<2

4. Feed rate

   The feed rate was optimized to control cold-cap coverage during the test. Changes in feed rate were required to maintain system stability and to keep parameters listed in Table 4.1 within target range.

5. Processing rate and cold-cap coverage

   Maximum steady-state processing rates were established. The targeted cold-cap coverage was 85% to 95%. To achieve specific processing rates of 0.7 MT/d/m^2 to 1.1 MT/d/m^2 of glass, the feeding rates were maintained within a range from 1.3 to 2.1 kg/h.

6. Plenum temperature

   The target plenum temperature range under steady feed operation was 500 ± 150 °C. Feed rate, kiln temperature, and bubbling rate were all used to control the steady-state plenum temperature during the test.

7. Off-gas temperature

   Post-film-cooler unquenched off-gas temperature was constrained at <350 °C. The film-cooler air injection flow rate was the primary control for off-gas temperature. In addition,

adjustments of kiln temperature and feed rate were also used to control the off-gas temperature.

8. EVS temperature

   The EVS scrubbing solution was maintained at 30–45 °C. The scrubbing liquid was initially tap water, and it increased in volume with the collection of melter condensate and particulate emissions.

4.3 Surrogate Waste Feed Preparation

Table 4.2 summarizes composition of the high-Fe-Ni borosilicate glass for the RSM test. The feed to make this glass was prepared from AZ-101 waste simulant (a substitute for actual HLW from Hanford Tank 241-AZ-101), which was supplied by Noah Technologies Corporation in San Antonio, Texas. The waste loading for this waste is predicted to be limited by spinel formation. Table 4.3 shows the quantity of AZ-101 simulant and additives (glass formers and additional components) to produce feed.

Table 4.2. Composition of High-Fe-Ni Borosilicate Glass in Mass Percent of Oxides and Halogens

Component	Mass %	Component	Mass %
Al_2O_3	7.84	P_2O_5	0.31
BaO	0.09	SiO_2	38.47
B_2O_3	7.63	SO_3	0.08
CaO	0.54	TiO_2	0.03
CdO	0.62	ZnO	0.02
Cr_2O_3	0.16	ZrO_2	3.97
F	0.01	Cl	0.02
Fe_2O_3	17.5	Ce_2O_3	0.19
K_2O	0.32	CoO	0.01
Li_2O	1.90	CuO	0.04
MgO	0.12	La_2O_3	0.22
MnO	0.33	Nd_2O_3	0.17
Na_2O	17.81	SnO_2	0.10
NiO	1.50		

Table 4.3. Composition of Feed for Production of High-Fe-Ni Glass

Feed Component	Target Mass (g)	Actual Mass (g)
AZ-101 simulant	229,064	229,064
H_3BO_3	23,220	23,220
Fe_2O_3	12,560	12,560
NiO	1860	1860
Li_2CO_3	8600	8600
Na_2CO_3	47,250	47,250
SiO_2	62,750	62,750
H_2O	154,618	123,891
Total	539,922	509,195

The AZ-101 simulant arrived in two partially filled 55 gallon drums. A significant amount of solid/liquid separation was noted for both drums. The slurry in each drum was first homogenized by manual mixing with a paddle before it was pumped into one large polyethylene container and mixed with a dual-blade impeller for ~1.5 h. Then, the glass formers and other additives were added over a period of 4 h while the mixture was continuously agitated with the impeller. Additions to the AZ-101 simulant were made in the following order: Na_2CO_3, Fe_2O_3, NiO, Li_2CO_3, H_3BO_3, SiO_2, and H_2O. Since a workable viscosity of the feed was achieved with ~80% of the targeted mass of water, no additional water was added. The homogenized feed was transferred into three 55 gallon drums with protective liners for storage and transportation to PDL-E. A fraction of one drum was pumped into the feed tank of the RSM at the beginning of the test. Additional feed was transferred into the feed tank as needed, until all the feed was consumed and the test was completed.

Table 4.4 shows the results of chemical analysis for three glass samples collected during glass pouring compared to the target glass composition. The first sample represents the composition

of glass used to start this RSM test (crushed high-Fe-Ni glass from a previous RSM test). The second sample represents glass produced from the feed for this test; it was collected just before the beginning of the first idling. The third glass sample was collected before the third idling started with the purpose to validate production of a target glass composition (good mixing of the feed in the tank before it was charged into the melter). The glass compositions are in good agreement with target values. Concentrations of major components are within the error of the analysis. The higher concentrations of SnO_2 and SO_3 can be explained by the presence of impurities in the chemicals used to batch the RSM feed. The lower-than-target concentrations of Cr, Mn, and Ni are the result of spinel precipitation from glass. The spinel accumulates at the bottom, and the glass is depleted in spinel-forming components. The lower-than-target concentration of ZrO_2 in the glass can be explained by a possibly higher-than-tabulated concentration of water in zirconium oxynitrate hydrate, $ZrO(NO_3)_2 \cdot xH_2O$.

Table 4.4. Composition in Mass% of Oxides for Actual Glass Samples (1–3) Compared to Target Glass Composition

	Target	Sample 1		Sample 2		Sample 3	
Components	mass%	mass%	RPD (%)	mass%	RPD (%)	mass%	RPD (%)
Al_2O_3	7.84	7.78	−0.7	7.56	−3.6	7.56	−3.6
BaO	0.09	0.07	−27.3	0.07	−26.4	0.07	−24.7
B_2O_3	7.63	8.07	5.7	8.37	9.7	8.89	16.5
CdO	0.62	0.64	2.9	0.63	2.1	0.62	−0.1
CaO	0.54	0.58	7.0	0.49	−8.8	0.48	−10.6
Cr_2O_3	0.16	0.14	−12.7	0.14	−11.7	0.14	−13.4
CoO	0.01	0.01	−31.6	0.01	−34.6	0.01	−18.9
CuO	0.04	0.03	−22.4	0.03	−23.6	0.03	−21.8
Fe_2O_3	17.50	17.80	1.7	17.59	0.5	17.59	0.5
La_2O_3	0.22	0.25	11.4	0.25	15.7	0.23	2.9
Li_2O	1.90	1.93	1.5	1.95	2.5	1.97	3.7
MgO	0.12	0.11	−8.4	0.12	−2.9	0.10	−14.2
MnO	0.33	0.29	−12.9	0.28	−14.3	0.28	−15.9
NiO	1.50	1.44	−3.7	1.37	−8.4	1.39	−7.5
P_2O_5	0.31	0.21	−33.3	0.26	−17.2	0.25	−20.2
K_2O	0.32	0.13	−57.8	0.14	−56.7	0.15	−53.3
SiO_2	38.47	36.80	−4.3	36.15	−6.0	36.58	−4.9
Na_2O	17.81	18.06	1.4	18.06	1.4	18.33	2.9
SO_3	0.08	0.12	45.8	0.13	64.2	0.13	67.3
SnO_2	0.10	0.18	75.8	0.19	89.2	0.17	67.6
TiO_2	0.03	0.03	−16.0	0.02	−17.7	0.02	−20.5
ZnO	0.02	0.02	1.8	0.02	4.6	0.02	−0.4
ZrO_2	3.97	3.21	−19.2	3.16	−20.4	3.16	−20.4

5.0 Test Description

This section summarizes operation of the RSM to satisfy the test objectives, and includes a melter post-test inspection focused on the long-term performance.

5.1 Melter Operation

The melter was loaded with 4 kg of previously melted and crushed high-Fe-Ni glass and then heated by the kiln and the pour spout heaters. Joule heating was initiated after the middle kiln thermocouple read 902 °C and the melter electrode thermocouple was at 798 °C. The melter was at 1150 °C after 49 min. Charging of the feed into melter was initiated after 72 min at 1150 °C. A total of 509 kg of feed was processed during the test, producing 159 kg of glass.

During start-up of the melter, erroneous temperature readings were observed on several thermocouples monitoring the pour spout, kiln, off-gas, and process water temperature. This was corrected by providing a stable electrical ground for all affected thermocouples. There were no further problems with temperature readings throughout the duration of the test.

The glass was melted under the operational targets that were previously discussed in Section 4.0. Several charts are provided below to graphically represent the actual operating conditions during the test. A summary of the main operating parameters is given in Table 5.1.

Table 5.1. Summary of RSM Operations

Start date	2/29/2016
Start time	10:25 a.m.
Total hours of operation	1895
Avg. plenum temperature during feeding/pouring (°C)	575
Avg. melt temperature during feeding/pouring (°C)	1149
Bubbling rate (slpm)	1.4
Avg. steady-state feed rate (kg/h)	1.76
Max. sustained production of glass (kg/day/m^2)[(a)]	1130

(a) Rate calculated from feed data based on surface area of the melt and best feed rate that was maintained for more than 5 h.

The temperatures of the glass pool were relatively stable, with a standard deviation of less than 10.3 °C from the target of 1150 °C over the course of feeding/pouring. The temperature of the thermocouple adjacent to the bubbler was generally lower. This difference was attributed to the cooling effect of air bubbles. The plenum temperature ranged from 515 to 622 °C during steady-state operation, which was within the targeted temperature range of 500 to 700 °C. The maximum steady-state feed rate was 2.6 kg/h and occurred during the 10th feeding/pouring cycle. The average feed rate was 1.76 kg/h. The feed rate was regularly adjusted to maintain cold-cap coverage of 85 to 95%. The temperatures of the melt at each electrode and plenum temperatures were recorded throughout the duration of the test and are shown in Figure 5.1. Higher plenum temperatures occurred during idling periods due to the absence of feed charging into the melter. The temperature spike of 1210 °C observed during 7th feeding/pouring period

was the result of two overfeeding incidents (discussed in Section 5.2) when the thermocouples were no longer immersed in molten glass and the DAC system was trying to maintain the temperature of the glass pool at 1150 °C.

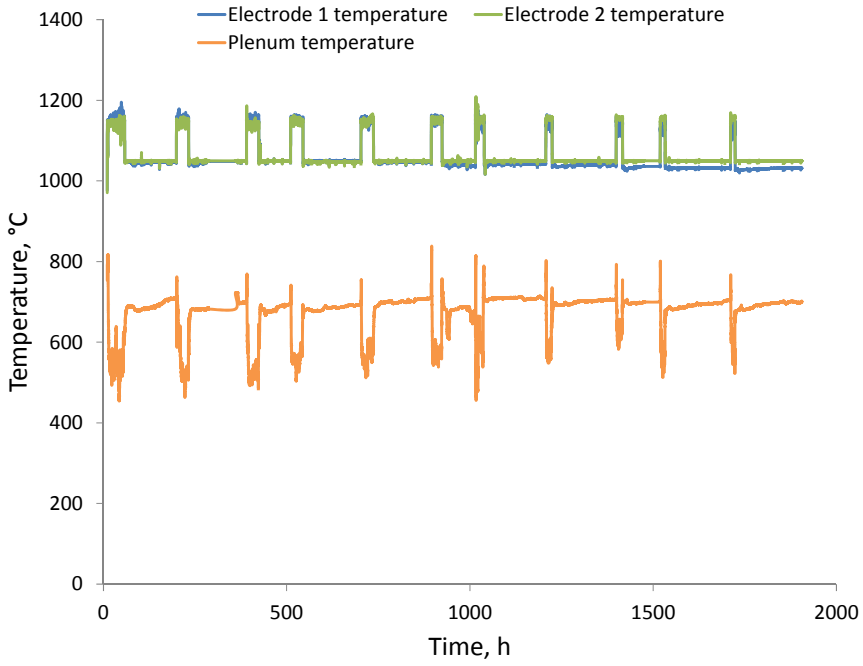

Figure 5.1. Temperature History for the Bulk of the Melter (Electrodes 1 and 2) and Plenum Space

The average supplied power to the melter for each feeding/pouring period was 2.94 kW with a standard deviation of 0.55 kW, indicating good temperature control without large swings in electrode power. Large deviations in electrode power were only observed twice. These deviations occurred during the 7th feeding/pouring period when overfeeding of the melt crucible resulted in the majority of the glass being discharged into the glass canister in a relatively short period of time. The overfeeding was the result of a faulty latch on the peristaltic feed pump head, which was subsequently replaced and caused no further operational problems. The faulty latch allowed the feed recirculation pump to briefly take control of the feed rate. This brief spike in feed rate caused a large amount of feed to be dumped into the melter, and led to an increase of the gravity-induced pressure, followed by a sudden discharge of molten glass. The reduction of glass coverage over the electrodes after this accident resulted in significant changes in the voltage and current. However, overall good control of electrode power was maintained for the remainder of the test. Electrode current and voltage history are shown in Figure 5.2. Electrode power is shown in Figure 5.3. The electrode power spike above 8 kW is the result of the overfeeding of the melt crucible. Figure 5.4 shows the electrode power history in relation to the melt-crucible and plenum temperatures. The drop in the melter power during idling periods occurred during conductivity measurements, when power to the electrodes was turn off.

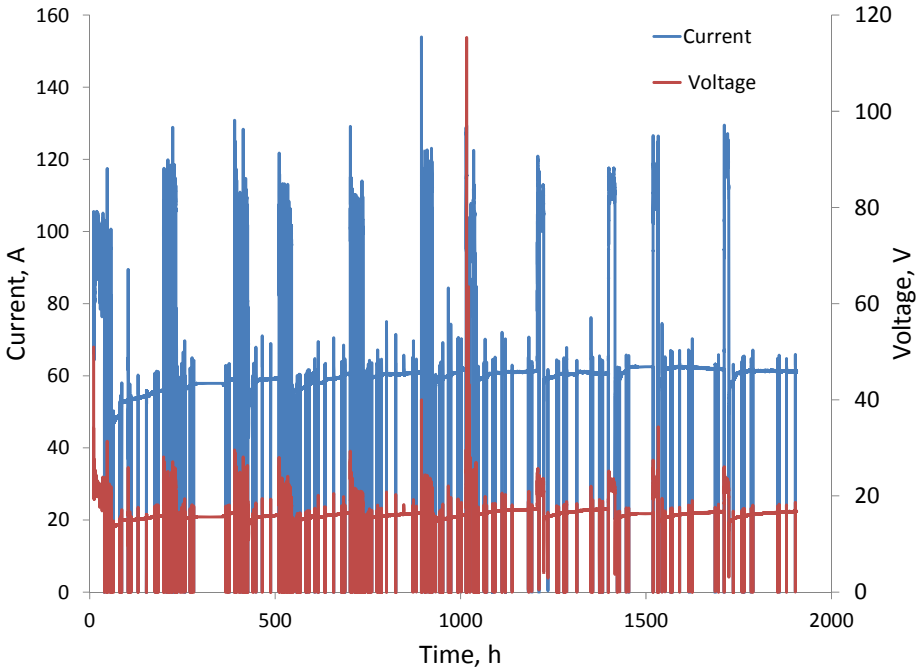

Figure 5.2. Current and Voltage Profiles Maintained throughout the Test

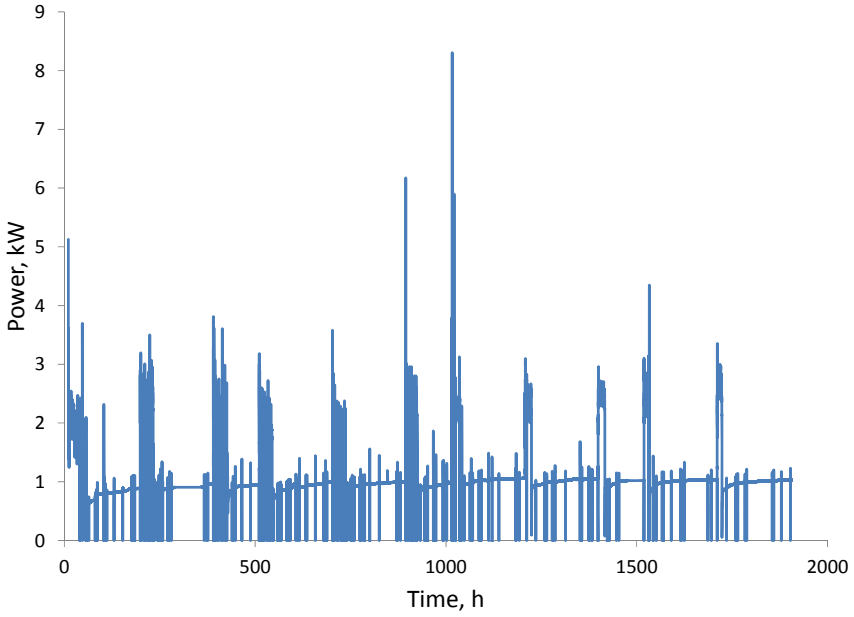

Figure 5.3. Electrode Power Profile Maintained throughout the Test

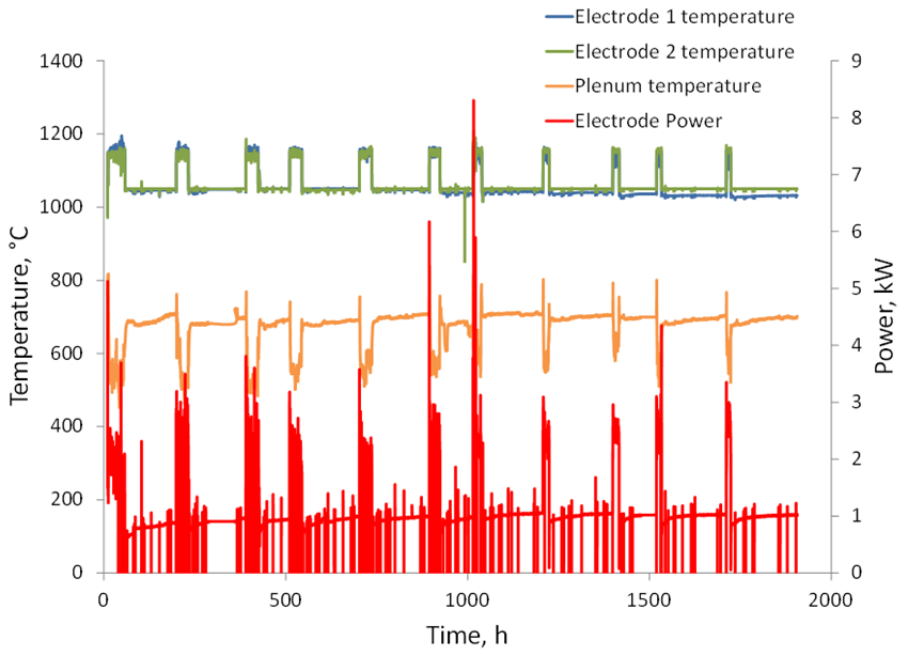

Figure 5.4. RSM Power Profile and Temperature History for the Bulk of the Melter (Electrodes 1 and 2) and Plenum Space

5.2 Melter Feeding

Feed-line and nozzle plugging occurred frequently during the first feeding/pouring period of the test. Regular cleaning of the feed nozzle was required, and the feed rate was steadily reduced from the beginning to the end of the first feeding/pouring period to minimize clogging. These problems were attributed to insufficient mixing of feed prior to melter start-up. Continued agitation of the feed in the feed tank during the first idling period was sufficient to eliminate this problem. From then on, only occasional partial nozzle clogging occurred. Interruptions in the delivery of feed to the melter totaled ~4 h over the course of the test. This downtime included 23 min to remove and replace a ruptured feed pump hose. To prevent this from recurring, the feed and recirculation pump hoses were replaced after each feeding/pouring cycle, which proved to be sufficient.

An average feed rate of 1.76 kg/h was maintained with minor adjustments throughout the remainder of the test. The highest steady-state feed rate, 2.6 kg/h, was achieved near the end of the test during the 10th feeding/pouring period. This was an inevitable effect of replacement of the old bubbler with a new one while keeping the cold-cap coverage within the target range of 85 to 95%. This cold-cap coverage was maintained during the majority of the test, and addition of feed can be correlated with changes in plenum temperature.

The melter feed rate over the duration of the test is shown in Figure 5.5. The two large pours caused by faulty latch on a peristaltic pump that occurred during the seventh feeding/pouring period are indicated by the temporary spike in the feed rate. In connection with this incident, the temperature in the 30° sloped section of the riser briefly spiked to 1290 °C (as shown in Figure 5.8). This important observation needs to be emphasized, because a vigorous discharge of molten glass together with an increased temperature of poured glass removed layers of

spinel that had accumulated over seven idling periods. More detailed information on the accumulation of spinel crystals is provided in the Section 6.0, “Data Analysis Results and Discussion”.

For the first large pour, ~3.3 kg of feed was pumped into the melter over a period of 7 min (with an average feed rate of 473 g/min) before the problem was observed and feeding stopped. The weight of the extra feed on top of the melt resulted in an uncontrolled pour of glass. About 2.7 kg of glass (~60% of glass inventory) was discharged and collected during that time. Then, the melter was fed normally at a feed rate of ~30 g/min for about 5 h and attempts were made every hour to pour glass without success; the melter had not recovered yet from the overfeeding incident. Approximately 7.7 kg of feed was charged into the melter during this 5 h period; then, the hose latch on the small peristaltic pump failed again, being not fully locked, and caused a second uncontrolled pour of glass. This time approximately 1.4 kg of feed was charged into the melter over a period of 12 min (with an average feed rate of 117 g/min) and resulted in 3.47 kg of glass (~77% of glass inventory) in the canister. After the second large pour event, pouring was attempted every hour without any success. The normal pouring operations resumed after ~6 h. To prevent operational problems with the hose latch on the small peristaltic pump, the faulty latch was replaced at the conclusion of the seventh feeding/pouring period, which was sufficient to prevent this from happening again.

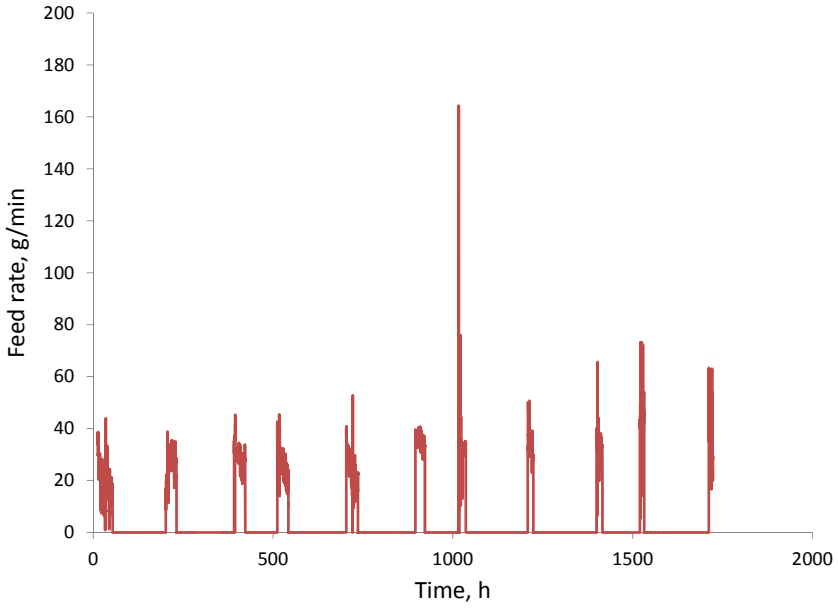

Figure 5.5. RSM Feed Rate Profile. Each data point represents an average rate over a period of 30 min

5.3 Melter Bubbling and Off-Gas

The RSM used a bubbler throughout the feeding periods for the duration of the test. The old bubbler, used in previous RSM tests, failed at the end of the fifth feeding/pouring cycle because of corrosion that occurred ~1.9 cm below the surface of the melt pool. Replacement with a new bubbling tube resulted in a noticeable increase in processing rate. This suggests that air may have been leaking in the corroded section of the original bubbler over a number of previous

feeding/pouring periods, affecting the feed processing rate. The bubbling rate throughout the duration of the test is shown in Figure 5.6. The average bubbling rate was 1.4 slpm.

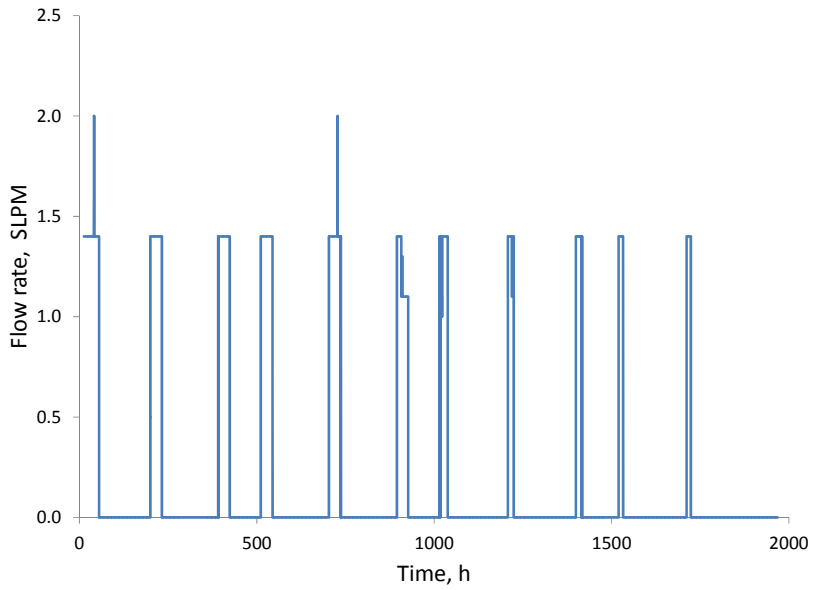

Figure 5.6. RSM Bubbling Rate Profile

The melter off-gas system was operated within target temperature range for each off-gas location. The film cooler off-gas temperature experienced the most variability. Its temperature profile is shown in Figure 5.7. Off-gas temperature was controlled by adjustments of flow rate of cooling air to the film cooler and by adjustments of feed rate. The primary challenge during this long-duration test proved to be maintenance of the melter off-gas system. Regular plugging of the film cooler began to occur during the ninth feeding/pouring cycle and continued throughout the duration of the test. The film cooler required regular—hourly in some cases—cleaning to maintain target system vacuum conditions and proper system operation. The location of the open hole in the cold cap in relation to the location of the exhaust and feed nozzle appeared to affect the number and frequency of film cooler cleanings required. This suggests that splashback from the feed in the cold-cap region was a major contributor to film cooler clogging.

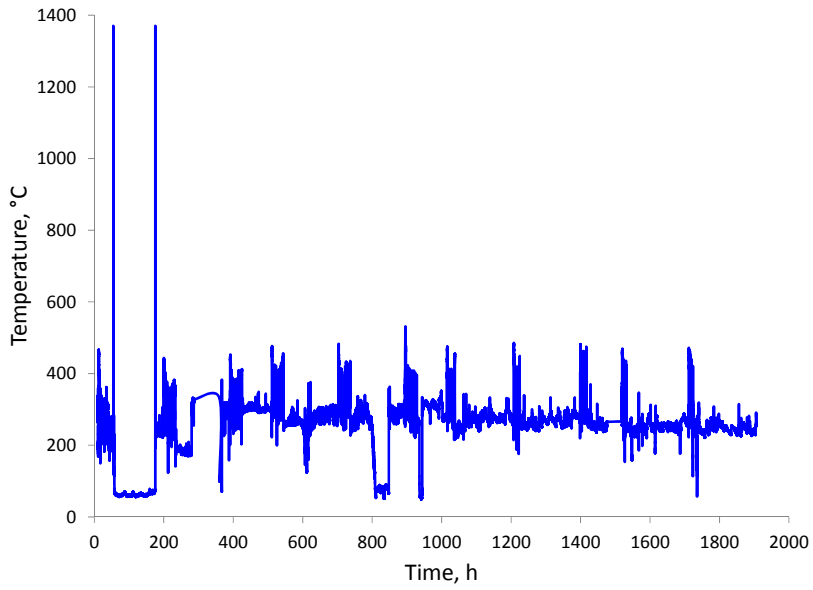

Figure 5.7. RSM Off-Gas Temperature Profile

In addition to problems with the film cooler, deposits inside of the main control valve located downstream of the HEME in the off-gas exhaust system proved problematic. Periodic cycling of the control valve from 100% open to closed on a fairly regular basis was required to maintain proper control valve operation. The control valve problem primarily occurred during idling when the melter was kept under low vacuum over extended periods of time. The control valve would slowly drift from approximately 60% open to near 100% open to maintain 0.1 in. WG vacuum. It was noted that this problem occurred more frequently as the concentration of solids in the EVS solution and its volume increased over the course of the test. After maximum tank capacity was reached in the EVS tank, the EVS solution was removed and replaced with clean tap water. The addition of clean tap water to the EVS tank resulted in an immediate decrease in control valve problems during subsequent idling periods. This suggests that the valves located downstream of the EVS system are sensitive to the concentration of off-gas contaminants in the scrubber solution.

5.4 Melter Idling

Each feeding/pouring period was followed by an idling period of 4 to 7 days. The length of each idling period was adjusted to allow for each feeding/pouring period to begin any weekday from Monday to Thursday of each week. Feeding was stopped and the cold cap was allowed to melt off before the melter was set to the idling condition. All feed lines were flushed with a small amount of water after feeding was stopped. The film cooler was subsequently cleaned out and the melt temperature was decreased from 1150 °C to 1050 °C after the cold cap disappeared. As the melter temperature dropped, the pour spout heaters were turned off and the kiln temperature was increased to 900 °C to prevent the temperature in the glass-discharge riser section from decreasing too quickly. The vacuum to the melter was reduced to 0.1 in. WG once the pour spout temperature was low enough to prevent glass discharge under the lower vacuum condition. Lastly, the EVS system and its associated chiller were turned off for the duration of the idling period. Cooling air to the film cooler was reduced to a lower rate than the one used during feeding/pouring periods. These melter vacuum and exhaust conditions were maintained

for the duration of the idling period. Treatment of the melter exhaust stream during each idling period was performed for the film cooler and the HEME.

Previous RSM tests have shown that a temperature of 935 °C in the 30° sloped section of the glass-discharge riser corresponds to a temperature of 870 °C at the bottom of the vertical section of the glass-discharge riser. Frequent adjustments were made to the set point of kiln temperature while the melter was cooling down to 1050 °C to reach the target of 935 °C in the sloped riser section. Additional adjustments were made during the course of each idling period to maintain this temperature. During the fourth idling period, the seal between the glass-discharge canister and the bottom of the melter was lost overnight due to a leaking hydraulic valve in the jack used to support the glass-discharge canister against the bottom of the melter. The temperature in the sloped section of the glass-discharge riser during this time briefly dropped to 905 °C. A mechanical jack was installed and used as a backup to the hydraulic jack during future idling cycles to prevent recurrence of this problem. The glass-discharge riser at the center of the 30° sloped section was maintained at an average temperature of 936.3 °C over a period of 1204 total hours of idling. Glass-discharge riser and melter temperatures for the whole test are shown in Figure 5.8.

Figure 5.8. Temperature Profiles for Melter and 30° Sloped Section of the Riser

5.5 Melter Post-Test Inspection

At the conclusion of the test, the power was turned off to the melter electrodes, the surrounding kiln, and the pour spout heaters. The melter electrodes and bubbler were removed from the melt while the glass was molten and retained for future inspection and/or use. The melt was subsequently quenched by feeding water into the melter via the feed nozzle until the water completely covered top of the glass in the melt crucible. After quenching was completed, all systems were shut down and the melter was allowed to cool to room temperature. This took about three days. Then, the melter was disassembled for inspection.

Figure 5.9 and Figure 5.10 show melter electrodes after the test. The electrodes were discolored but did not show signs of heavy corrosion. However, there was some oxidation and evidence of small pits on the surface. The Inconel 690 bubbler (replaced at the end of the fifth feeding/pouring cycle) showed no sign of corrosion or structural damage. Figure 5.11 and Figure 5.12 show the top and bottom of the lid of the RSM, respectively. Figure 5.12 also shows the location of each melter component within the lid area for reference. Inspection of the lid revealed a significant amount of material adhered to its underside. The deposits appeared to be sintered feed and glass from back-splash during feeding. Also included were deposits that originate from volatilization of components such as Na and B during idling periods. Figure 5.13 shows the top of the melt after quenching.

Figure 5.9. Back of Melter Electrodes (Facing the Wall of the Crucible) after Their Removal from Molten Glass

Figure 5.10. Front of Melter Electrodes (Facing the Center of the Crucible) after Their Removal from Molten Glass

Figure 5.11. Top of RSM Lid after Test

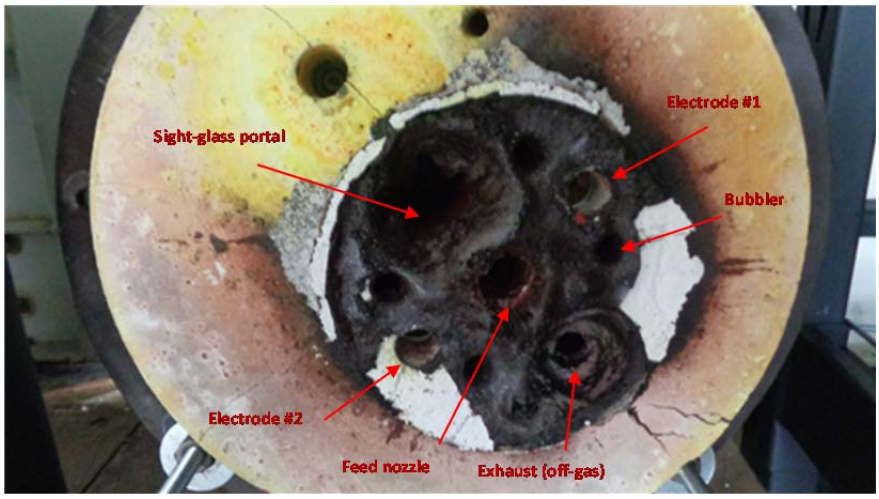

Figure 5.12. Bottom of RSM Lid after Test

Figure 5.13. Top View of Melt Pool after Quenching (After Completion of the Test)

All sections of the off-gas system were disassembled and inspected. Loose off-gas deposits were removed and weighed. Off-gas deposit samples were collected from the film cooler, the 90° bend in the off-gas tube above the melt chamber, the long tube downstream from the 90° bend, and the exhaust pipe entering the EVS system. The locations of each of the off-gas sections within the RSM system are shown in Figure 5.14. Pictures of deposits for selected sections are shown in Figure 5.15, Figure 5.16, and Figure 5.17. In total, 660 g of solid deposits were collected in the off-gas pipes of the RSM system after 11 weeks of operation. The particulate off-gas deposits represent 0.13 wt% of the total liquid feed and 0.3 wt% of the solid feed components. Off-gas deposits were observed in all off-gas component sections. However, they were particularly high in the areas where the flange of one off-gas pipe section was connected to the flange of another section. This suggests that welded joints in the pipes may be more efficient than flanged joints at preventing the accumulation of deposits and avoiding obstruction of the off-gas system. In addition, noticeably more deposits of particulate material were found in the cooler sections of the off-gas system.

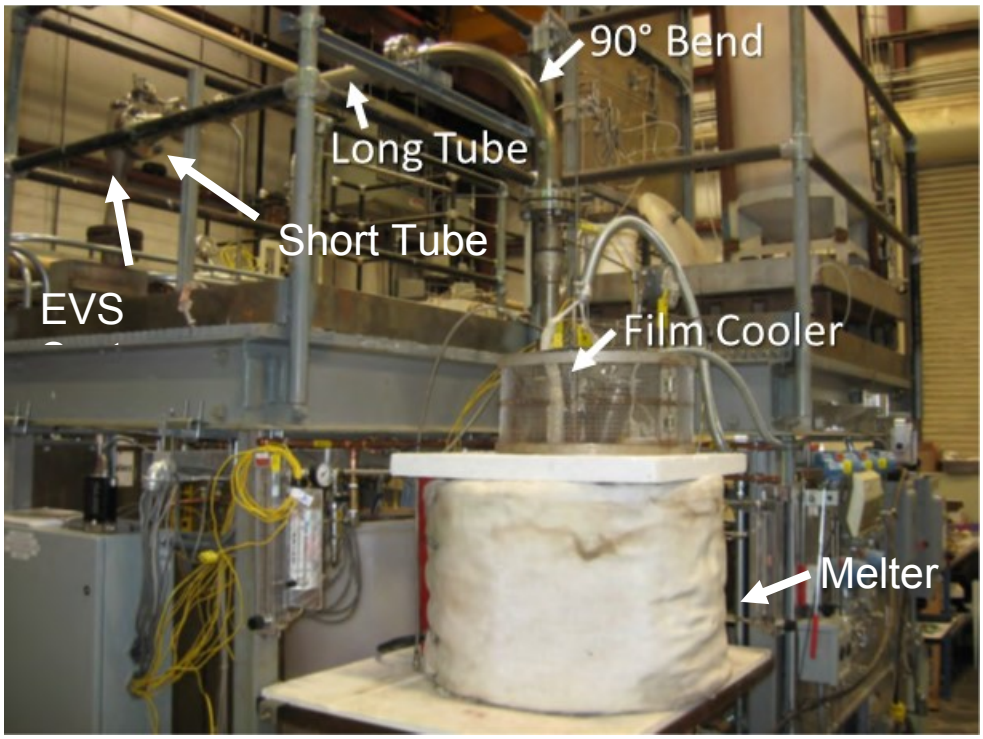

Figure 5.14. Areas in Off-Gas System with Solid Deposits

Figure 5.15. Off-Gas Deposits in the Film Cooler

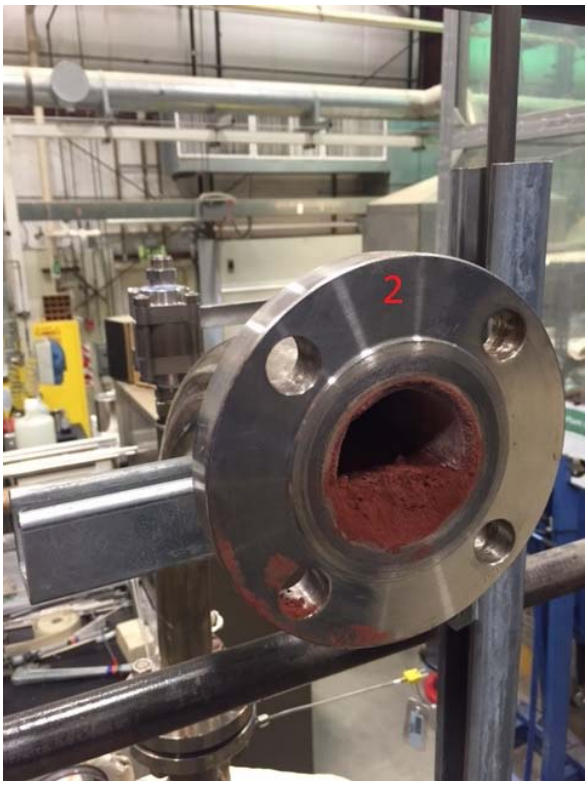

Figure 5.16. Off-Gas Deposits in the 90° Bend Downstream of Film Cooler

Figure 5.17. Off-Gas Deposits at the Entrance to the Ejector Venturi Scrubber (EVS) System

5.6 Melter Dissection

The melting crucible and pour spout were filled with epoxy prior to melter dissection. After the epoxy had cured, the Inconel shell surrounding the melter was removed. Figure 5.18 shows the Alfrax refractory surrounding the melt chamber and the location of the pour spout. Cracks observed in the Alfrax refractory developed after testing was completed. They were a result of rapid quenching with water. The melting crucible was subsequently separated from the Alfrax refractory and cut in half. The center of the pour spout cross-sectional area was targeted to be the center of the cut.

Figure 5.18. Alfrax Refractory (Beige Color) Surrounding the RSM

Figure 5.19 shows a cross section of the melter before additional cutting and polishing, showing details of the melt pool and 30° sloped and vertical sections of the glass-discharge riser. Figure 5.20 shows polished cross sections of the bulk of the melter and the glass-discharge riser. Figure 5.21 shows a polished cross section of the opposite half of the glass-discharge riser. Significant accumulation of spinel crystals is evident in the bulk of the melter and in the 30° sloped and vertical sections of the riser. In the bulk of the melter, the thickness of the accumulated layer varied from 0.5 to 3.4 cm. Thicker deposits formed towards the wall of the melter due to bubble-induced currents from the bubbler and natural convection from temperature differences in the molten glass. In the glass-discharge riser section, a crystal bank ~1.4 cm thick formed at the entry point to the 30° sloped section, obstructing more than 60% of the opening (2.3 cm). Then, the layer thickness decreased to 1.2 cm and was nearly constant throughout. In the vertical section of the riser, the dead flow zone in the corner together with crystal accumulation resulted in a layer that obstructed about half of the opening.

Figure 5.21 shows the location of the conductivity probe along with the accumulated layer of spinel crystals. Both electrodes of the probe were buried in the accumulated spinel layer. Blockage of the riser was not achieved by the end of this test. However, two large pour events likely removed most, if not all, deposits accumulated over the period of seven idlings. Therefore, it is important to acknowledge that more than half of the riser opening was blocked by the accumulated layer of spinel crystals and that a thick layer formed in the bulk of the melter after just four idlings.

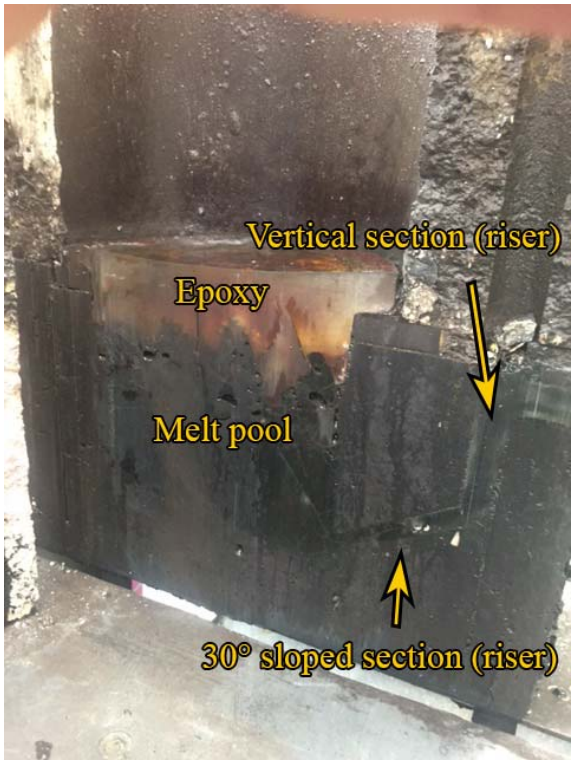

Figure 5.19. Cross Section of the RSM

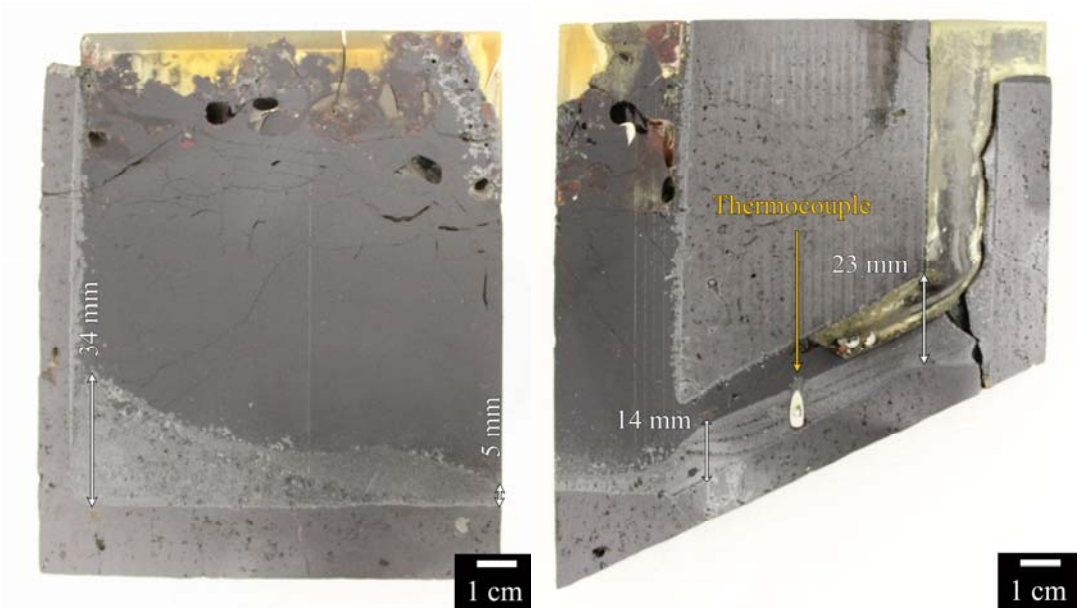

Figure 5.20. Polished Cross Sections of Bulk of the Crucible (left) and Riser of the Crucible (right) Showing Accumulated Layer of Spinel Crystals in These Sections. Also shown is the location of thermocouple in the 30° sloped section of the riser.

Figure 5.21. Polished Cross Section of the Other Half of the RSM Glass-Discharge Riser Section

6.0 Data Analysis Results and Discussion

6.1 Electrical Conductivity Probe

Prior to testing in the RSM, an electrical conductivity probe was developed and studied in the laboratory (Edwards et al. 2017). The probe was composed of two vertically configured parallel Pt electrodes, which allowed the resistivity of the glass melt to be determined:

$$\rho = RA/L \quad (1)$$

where ρ is electrical resistivity (Ω·m), A is the surface area of the electrodes (m^2), L is the distance between the electrodes (m), and R is the resistance (Ω). Combining L and A as a geometric constant (cell constant K), $K = L/A$, that is specific to each probe and can be determined from conductivity measurements of standard KCl solutions at room temperature, the conductivity of the glass melt (σ, $\Omega^{-1}\cdot m^{-1}$) can be calculated:

$$\sigma = 1/\rho = K/R \quad (2)$$

Figure 6.1 shows an example of the probe used for testing in the laboratory. The probe was constructed of an alumina sheath that was 42 cm tall and 4 mm in diameter with two Pt/10%Rh wires inside. A 4 × 4 mm paddle was welded to the bottom wire and represented the bottom electrode, and a bare wire represented the upper electrode. Measurements were collected using a potentiostat/galvanostat (Solartron 1470E) coupled with a frequency analyzer (Solartron 1400). The unique geometric property of each probe, the cell constant K, was determined using standard conductivity solutions. The small differences in K values (292–315 m^{-1}) and the ±10% agreement with certified conductivities of standard solutions provided confidence in the accuracy of the probes.

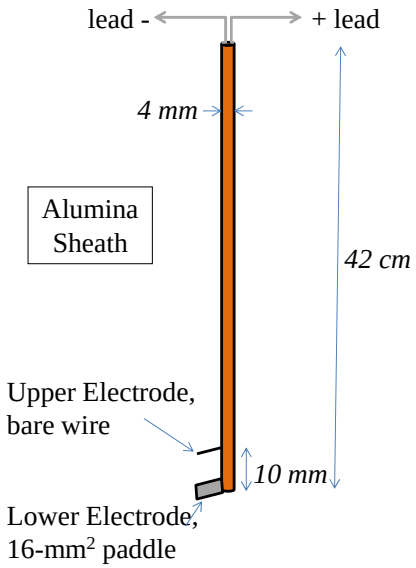

Figure 6.1. Design of Electrical Conductivity Probe

The laboratory testing of sodium silicate glass with and without accumulated layers of spinel crystals allowed for the determination of the conductivity of spinel crystals (σ_s) at specific temperatures, which are shown in Table 6.1. These crystals were precipitated from the high-Ni-Fe glass by heat treatment in a double crucible for 7 days at 850 °C. The crystals were recovered from the layer accumulated at the bottom of the crucible through overnight treatment with 20% HNO_3 heated to 60 °C to dissolve the glass, and then treated with 5% HF for 1 min to dissolve the residual silica gel. The morphology of the crystals is shown in Figure 6.2. X-ray diffraction of crystals confirmed trevorite ($NiFe_2O_4$) as the primary crystalline phase.

Table 6.1. Conductivity of Spinel Crystals at Different Temperatures

Temperature (°C)	σ_s (S/m)
875	31.13
850	29.93
825	26.81
800	23.83
775	21.89
725	17.34
675	12.19

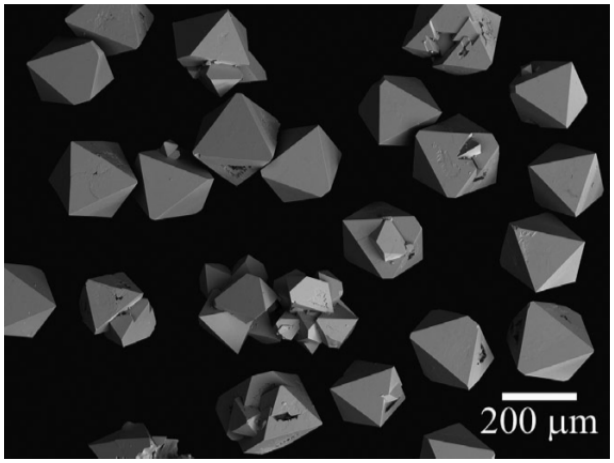

Figure 6.2. Scanning Electron Microscope (SEM) Image of Spinel Crystals

Figure 6.3 shows conductivities and layer thickness data as determined from two laboratory tests with high-Ni-Fe glass. Glass was melted at 1200 °C for an hour, to make sure it was crystal-free, before temperature was decreased to 850 °C. The glass was then idled at 850 °C for 5 days (Test 1) and 6 days (Test 2), with conductivity measurements collected every 12 minutes. At the beginning, the glass had a conductivity of ~17.5–18.5 S/m at 850 °C. Since the conductivity of the spinel at 850 °C (29.9 S/m) was higher than that of the glass at the same temperature, the gradual buildup of spinel crystals resulted in an overall increase of measured conductivities. Since the probe was composed of a flat plate on the lower electrode and a bare wire on the upper electrode, the electrical current passed through the glass/spinel layer in a three-dimensional, triangular path. Therefore, the change in conductivity would depend on the volume of the spinel layer within that electrical path. This relationship can be described with Equation 3:

$$\sigma_s(V_s/V) + \sigma_g(V_g/V) = \sigma_m \quad (3)$$

where V is the total volume between probe electrodes, V_s represents the volume occupied by spinel crystals, V_g is the volume occupied by the glass, σ_s is the conductivity of spinel at 850 °C, σ_g is the conductivity of the glass at 850 °C, and σ_m is the measured conductivity of the glass/spinel system at 850 °C. If crystals occupy the entire volume between electrodes, the layer will have a conductivity of 29.9 S/m; if there are no crystals, the layer will have the conductivity of high-Ni-Fe glass (18.5 S/m for 6 days idling test). Assuming these and using Equation 3 and the known distance between the upper and lower probe electrodes (10 mm), the thickness of a crystal layer between probe electrodes can be determined. The change in conductivity, from 18.5 to 19.6 S/m, for Test 2 indicated accumulation of crystals to a ~1.0 mm thick layer. Figure 6.4 shows that this value agreed well with a 1.1-mm layer as determined from a cross section of the glass and probe.

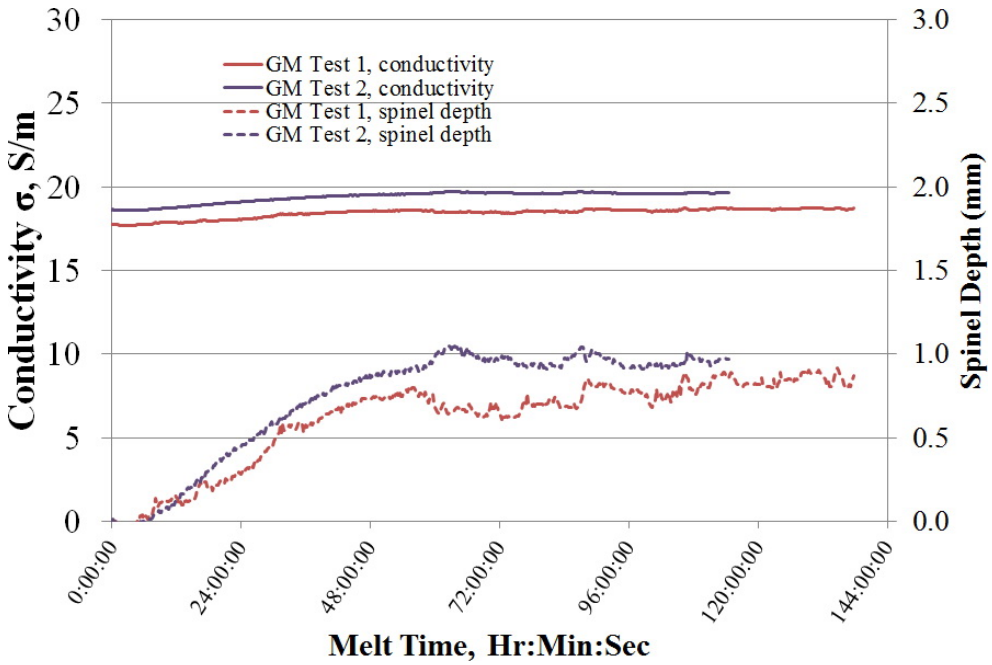

Figure 6.3. Conductivity and Layer Thickness as Function of Time for Lab-Scale Testing with High-Ni-Fe Glass

Figure 6.4. SEM Image of Accumulated Layer from Test 2 (850 °C for 6 days). The bottom electrode is white, spinel crystals are gray features, and glass is dark gray.

To validate lab-scale data, a probe was installed in the glass-discharge riser section of the melter in an attempt to monitor accumulation of spinel crystals in real time. The probe design for the RSM test was modified to include an alumina sheath 60 cm long. Electrical leads and probe electrodes were made with Pt-10%Rh wire. Both the upper and the lower electrodes of the probe were bare wires placed vertically 10 mm apart, extending 4 mm horizontally from the probe shaft (Figure 6.5).

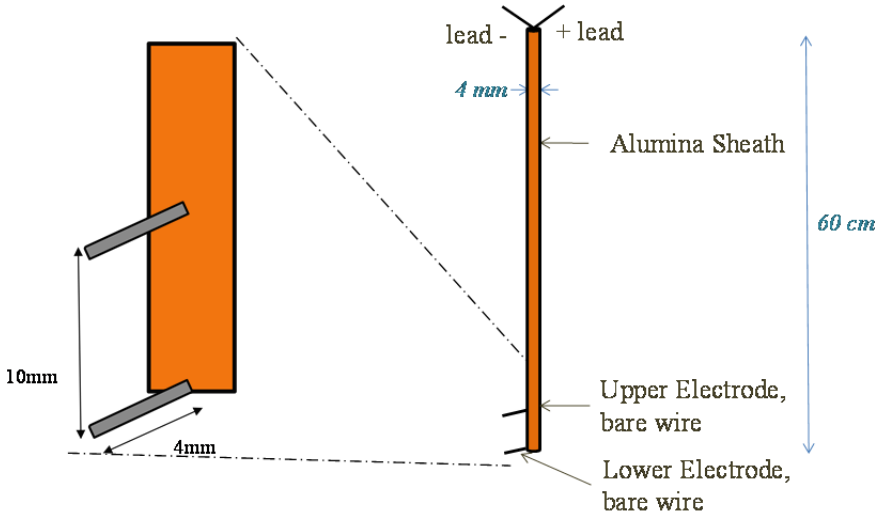

Figure 6.5. RSM Probe Design

The probe was calibrated before the test with standard conductivity solutions to obtain the cell constant (K value). The electrical conductivity data were collected with a Solartron 1470E potentiostat/galvanostat coupled to a Solartron 1400 frequency analyzer, which were placed on a platform adjacent to and above the RSM. The Solartron instruments and all associated wiring were shielded with high temperature insulation wool to minimize exposure to heat. The probe was placed into the riser with its electrodes facing the glass pool of the melter and secured in

place with a nut and a ceramic ferrule. The Solartron analysis sequence was set to be a 5 s open circuit followed by an impedance sweep from 101 to 106 Hz at a constant potential with 0 V of applied potential and 10 mV of AC amplitude. Two to six measurements per day were completed for each idling. For each measurement, the RSM power was turned off for approximately 2 min. Doing so effectively eliminated interference with melter electrodes.

Usually, two thermocouples are inserted into the riser of the melter to monitor temperature during pouring/idling. One is located at the center of the 30° sloped section and another at the bottom of the vertical section of the riser. However, with the probe in place, there was no longer enough space for a thermocouple in the vertical section of the riser. Therefore, temperature correlation data (sloped vs. vertical section of the riser) from previous RSM tests and a temperature from a thermocouple located in the sloped section were used to obtain/maintain required idling temperature at the bottom of the vertical section of the riser. The target temperature of 935 °C during idling for the sloped riser section corresponded to 870 °C at the bottom of the vertical section of the riser.

The results from the conductivity probe measurements for the first four idlings are shown in Figure 6.6. The higher conductivity for RSM glass (~22 S/m at 870 °C) compared to the conductivity of spinel-free glass (19.2 S/m at 870 °C) measured in the lab can be attributed to spinel crystals already present in this glass before idling started. The conductivity gradually increased after each idling, as indicated by red dashed lines (it increased from 19.2 to 26.9 S/m over four idlings). However, for each idling segment, the conductivity initially decreased before leveling off. This trend can be explained by settling of crystals that had been between the upper and lower electrodes. As the crystals settle, the volume of crystal-free glass between electrodes increases with time, which results in a decrease of conductivity. This decrease ends after most of the crystals are deposited at the bottom. Before another idling, crystals from the bulk of the melter are introduced into the riser section, increasing the conductivity between electrodes. Again, as they settle, the conductivity decreases with time due to increased volume of crystal-free glass until steady state is reached. Steady state for the next idling always has a higher conductivity than one from the previous idling due to increase in the thickness of the accumulated layer.

Figure 6.7 shows accumulation of the crystal layer over four idlings (24 days total) as calculated from electrical conductivity data. A linear fit of the data shows the layer growth rate to be ~0.346 mm/day. Extrapolating this rate for the total idling time of 66 days during this test, and assuming that the layer was not disturbed by pouring, a layer 22.8 mm thick can accumulate over that time. This layer would almost completely (99.5%) clog the riser opening (23 mm).

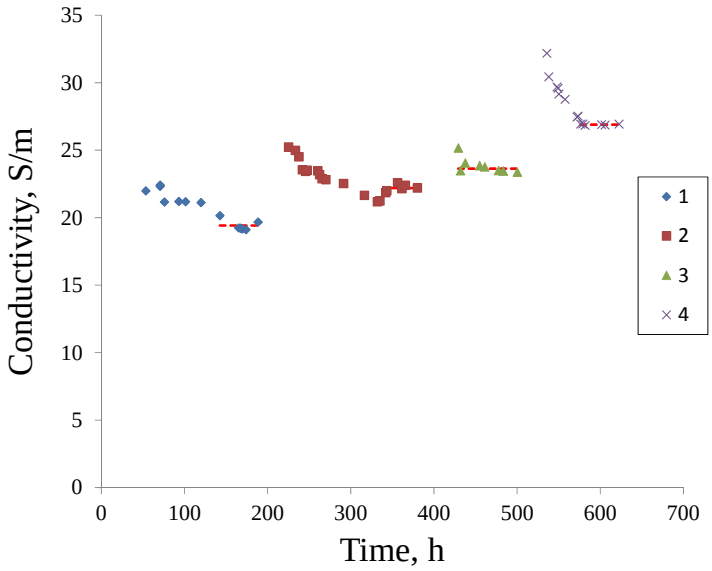

Figure 6.6. Electrical Conductivity over Time for First Four Idlings

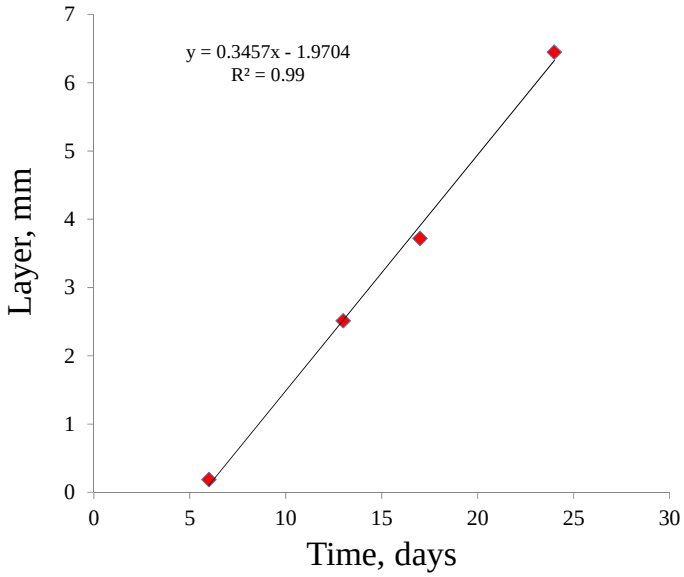

Figure 6.7. Thickness of Layer of Spinel Crystals Accumulated over Time for First Four Idlings as Depicted from Electrical Conductivity Data

The conductivity probe worked well for four idling periods. However, starting from the fifth idling period, the probe started to behave erratically. A large jump in conductivity occurred and probe conductivity significantly increased during each idling period. The probe stopped producing any useful data, although electrical conductivity data was regularly collected throughout the remainder of the test. It was hypothesized that a circuit existed between the conductivity probe electrodes and the melting electrodes. Both components are located at the bottom of their corresponding sections of the melter and would share a conductivity path if a continuous layer of spinel crystals was deposited on the bottom of the melter. Existence of a continuous layer was confirmed from the cross sections shown in Figure 5.20.

6.2 Disturbance of Settled Layer

Glass samples were collected during each pouring after idling and were analyzed for concentration of spinel crystals with XRD. This was done to evaluate the possibility of a partial or complete removal of crystal deposits accumulated during idling.

A total of 177 samples weighing from 53 to 115 g were collected and ground for 2 min in a tungsten carbide mill. Subsequently, ~1-g aliquots of glass powder were mixed with 5 mass% of CaF_2 (internal standard) for 1 min in a tungsten carbide mill and analyzed with a Bruker D8 Advanced x-ray diffractometer (Bruker AXS Inc., Madison, WI, USA) configured with a Cu Kα target (λ = 1.5406 Å) set to a power level of 40 kV and 40 mA, goniometer radius of 250 mm, 0.3° fixed divergence slit, and LynxEye™ position-sensitive detector with an angular range of 3°2θ. The scan parameters were 0.03° 2θ step size, 4 s dwell time, and 5 to 70° 2θ scan range. The detection limit of XRD for spinel was ~0.1 mass%. Bruker AXS DIFFRACplus EVA software was used to identify crystalline phases. TOPAS version 4.2 (Bruker AXS) software with a whole pattern fitting and trevorite structure file was used to determine concentration of crystals in the glass samples.

Figure 6.8 shows an example of how crystal content changed over time for glass samples collected every minute for 8 min after pouring was initiated: (1) after pour #1 (no idling, pour of previously melted and crushed high-Fe-Ni glass mixed with glass from feed) and (2) after pours #2–4, 8, 9, and 11, which occurred after idlings 1–3, 7, 8, and 10, respectively. The initial high concentration of spinel crystals in the glass for pours #1–3, 8, 9, and 11 can be explained by removal of crystals that were suspended in the glass or not fully embedded in an accumulated layer. After 2 min, the concentration of crystals in the glass reached the concentration of crystals in the bulk of the melter and remained about constant. The high concentration of crystals found in the glass samples from Pour #1 came from previously tested glass of the same composition. This glass was used to start joule-heated melting. The lowest concentration of crystals was found in the glass poured (Pour #4) after 4 days of idling (Idling #3). This suggests that short idlings of four days or less may not be detrimental to melter performance. More time is required for crystals to grow in the bulk and riser of the melter to produce glass with crystallinity of more than 0.5 mass% and to accumulate in the thick layer.

Figure 6.9 shows crystallinity variation in the glass samples collected later in the pouring events after different time intervals. Concentration of crystals in the glass varied from 0.2 to 3.9 mass%. At peaks, the concentrations are significantly higher compared to concentrations of crystals in the bulk of the melter, which varied from 0.3 to 1.1 mass%. This suggests that the accumulated layer may be disturbed and part of it removed during pouring.

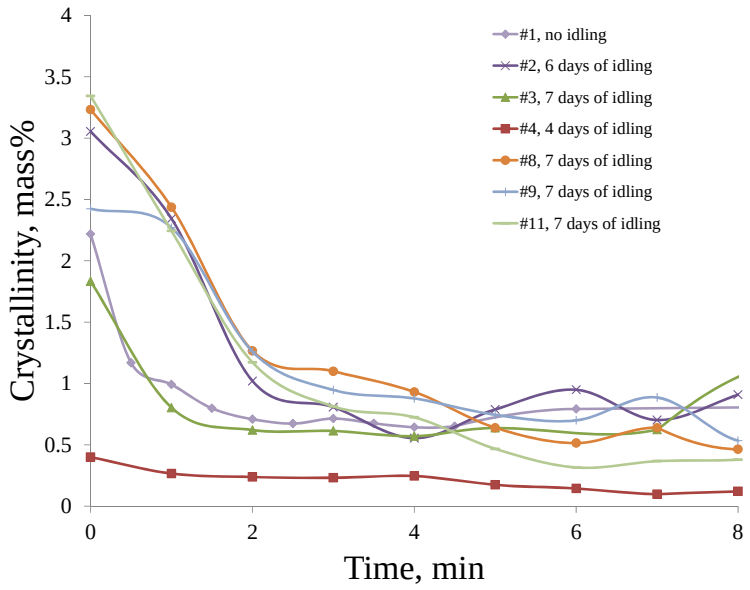

Figure 6.8. Concentration of Crystals in Glass Samples Collected during the First Eight Minutes for Seven Glass Pouring Events (#1–4, 8, 9, and 11)

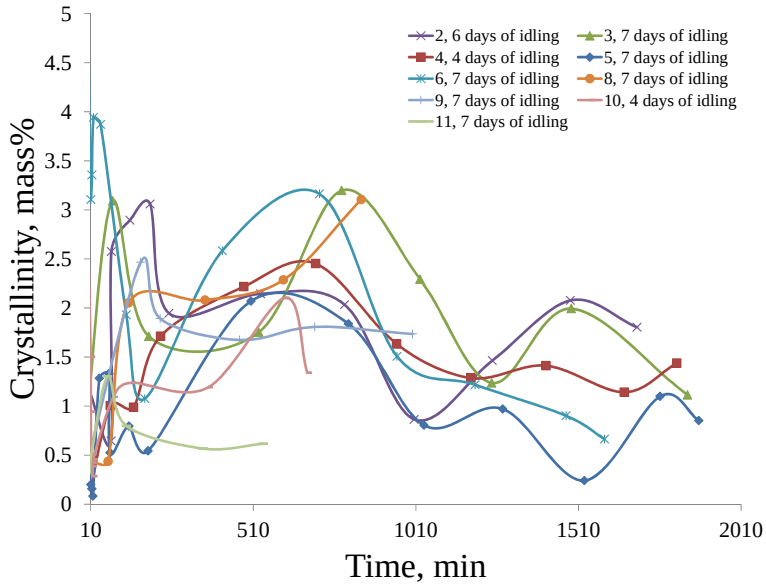

Figure 6.9. Concentration of Crystals in Glass Samples Collected at Later Stages of Glass Pouring Events #2–6, and 8–11.

6.3 Comparison of Crystal Layers Accumulated in Double Crucibles and RSM Melter

Figure 6.10 shows a layer of crystals accumulated in the 30° sloped section of the riser (complete views of the riser is shown in Figure 5.20 and Figure 5.21). A layer ~1.2 cm thick accumulated in this section. There are four distinct layers separated by bubbles, which may have formed through iron redox reaction when hot glass from bulk of the melter (1150 °C) came

in contact with cold glass in the riser (<950 °C). Considering previous RSM tests, each layer should represent one idling; four layers means four idlings. How is that possible, considering the melter was idled 11 times? This suggests that the two large and quite vigorous pouring events after Idling #7 (discussed in detail in Section 5.2) completely removed the layers of spinel accumulated over the period of seven idlings. Figure 6.11 shows in detail a part of a layer accumulated during Idling #8 and a part of the transition layer that formed during pouring (#9) of the glass (white-highlighted area in Figure 6.10). Clemex Vision PE 6.0 (Clemex Technologies Inc., Quebec, Canada) image analysis software was used to determine average crystal size and area fraction occupied by crystals in these two regions. The crystals that accumulated during Idling #8 had an average size of 44 μm and occupied 24.3% of the layer. In contrast, the transition layers with bubbles contained crystals with an average size of 27 μm, occupying 27.7% of the layer.

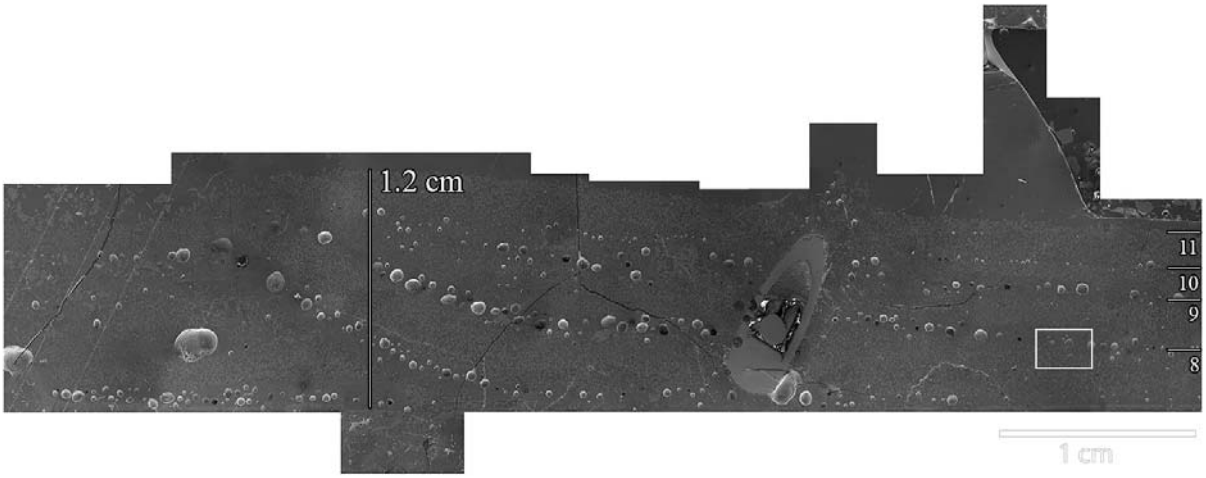

Figure 6.10. Stitch of SEM Images for Crystal Layer Accumulated in the 30° Sloped Section of the Riser during Period of Four Idlings (#8–11). The maximum layer thickness in this location was ~1.2 cm. Detail of the white-highlighted area is shown in Figure 6.11.

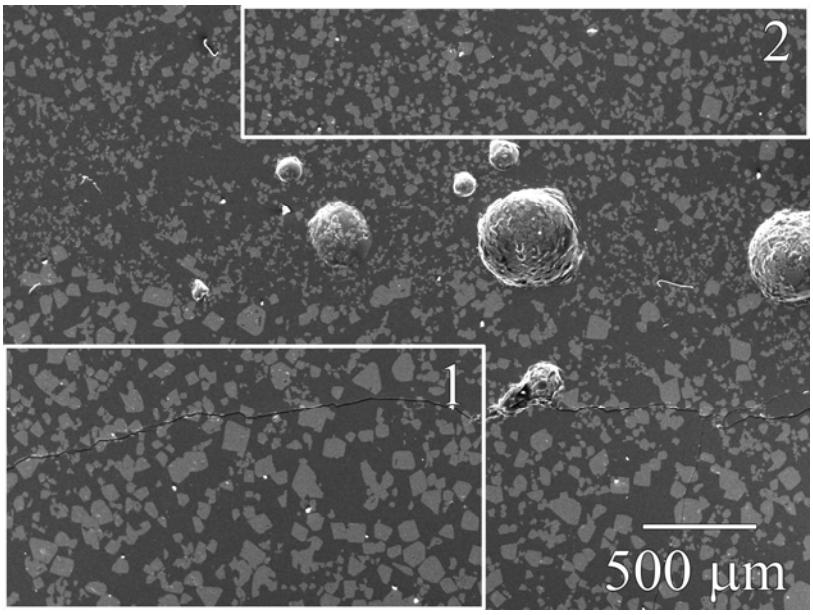

Figure 6.11. SEM Image of Crystals in the Accumulated Layer from the White-Highlighted Area in Figure 6.10. Average crystal size and fraction of crystals for Area 1 are 43.7 µm and 24.3%, respectively. Average crystal size and fraction of crystals for Area 2 are 26.9 µm and 26.9%, respectively.

Crystal accumulation in this glass (prepared from chemicals) was also studied in the laboratory using a previously developed double-crucible approach (Matyáš et al 2010, 2017). Glass powder was melted in a Pt crucible at 1200 °C for 1 h before being poured into three double crucibles that rested on a 0.5-m-diameter platform inside a Deltech furnace at 850 °C (selected to mimic temperature in the riser during idling). These double crucibles were covered with a ceramic lid and removed after 3, 6, and 8 days. Each crucible was air quenched and cross sectioned. Thin sections of the bottom were analyzed with scanning electron microscopy–energy dispersive spectroscopy (SEM-EDS), and Clemex image analysis software to determine the thickness of the accumulated layer and the shape, size, and surface fraction of spinel crystals in this layer.

Figure 6.12 shows SEM images of crystal layers that accumulated over time at 850 °C. Figure 6.13 shows thicknesses of layers for each dwell time as determined from image analysis. Extrapolation of a linear fit to the zero thickness layer shows that settling starts after ~40 h. The accumulation rate, 0.653 mm/day, is about two times higher than the one determined by electrical conductivity probe (0.346 mm/day) during the RSM test. The lower accumulation rate observed for the RSM test can be justified by small-scale removal of the layer during pouring. In addition, nonuniform temperature distribution in the riser, where temperature varied from 870 to 835 °C, sets up temperature-gradient convection, disrupting density-difference–driven settling of crystals. Furthermore, glass in the RSM test already contains small crystals of spinel before idling is initiated. These crystals act as nucleation sites, which would result in a high concentration of small crystals that settle slowly or, if smaller than 10 µm, remain suspended in the glass.

Table 6.2 shows thicknesses of accumulated layers, average crystal size, and crystal fraction in the layer for high-Fe-Ni glass processed in double crucibles at 850 °C for 3, 6, and 8 days.

Average crystal size and crystal fraction in the layer were 31 μm and 7.3%, respectively, after 3 days at 850 °C. The crystal size and crystal fraction increased to 74 μm and 25.4%, respectively, after three more days, (6 days total). Adding two more days, (8 days total), at 850 °C did not change the crystal size and crystal fraction much. They remained nearly constant with an average size of 72 μm and crystal fraction of 23.8 %. It should be noted that the crystals obtained from the double-crucible test are about 40% bigger than crystals observed in the layers with big crystals (43.7 μm) that formed during the RSM test. Crystal fraction in accumulated layers was about the same for double-crucible (23.8–25.4%) and RSM tests (24.4%).

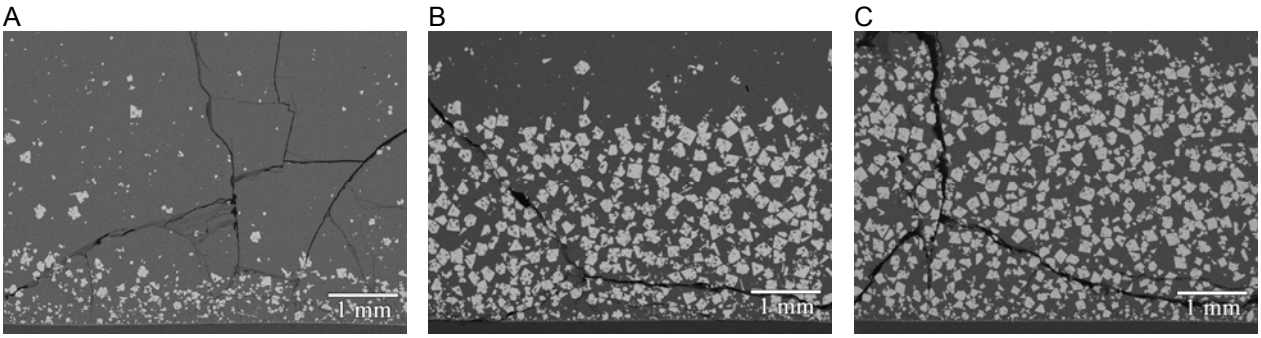

Figure 6.12. SEM Images of Crystal Layers Accumulated after 3, 6, and 8 Days at 850 °C in Double-Crucible Tests

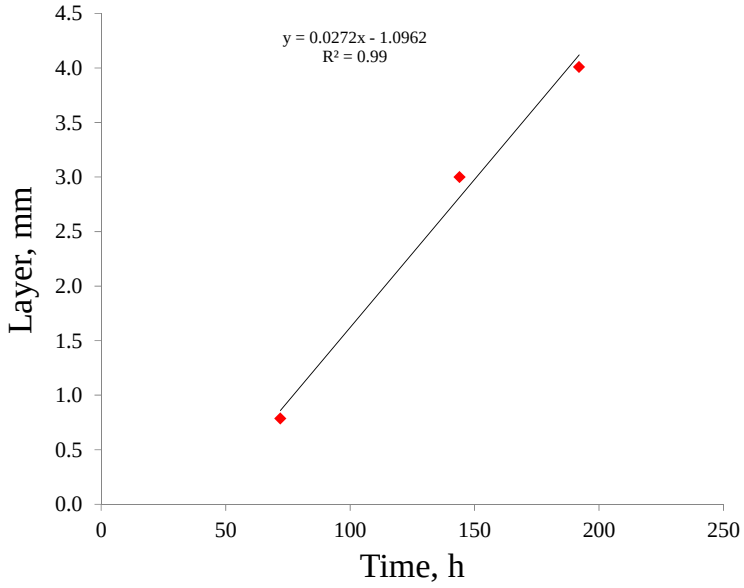

Figure 6.13. Thicknesses of Accumulated Layers as a Function of Time in Double-Crucible Tests

Table 6.2. Thickness of Accumulated Layers, Average Crystal Size, and Crystal Fraction for High-Fe-Ni Glass Processed in Double Crucibles at 850 °C for 3, 6, and 8 Days

Time (h)	Layer Thickness (mm)	Avg. Crystal Size (µm)	Crystal Fraction in Layer (%)
72	0.8	31.0	7.3
144	3.0	74.2	25.4
192	4.0	72.0	23.8

7.0 Conclusions

The RSM test validated the results obtained in the lab (Matyáš et al 2017). Compared to the lab-scale double-crucible test, smaller crystals formed and thinner layers accumulated during the RSM test. However, overall, a good agreement was found between lab-scale and RSM tests.

Two overfeeding incidents led to removal of layers of spinel accumulated over seven idling periods. In spite of that, a significant accumulation of spinel crystals occurred in the bulk of the melter and in the 30° sloped and vertical sections of the riser during the following four idling periods. In the bulk of the melter, the thickness of the accumulated layer varied from 0.5 to 3.4 cm. In the glass-discharge riser section, a ~1.4 cm thick crystal bank formed at the entry point of the 30° sloped section, obstructing more than 60% of the opening (2.3 cm). After that, the layer thickness decreased to 1.2 cm and was nearly constant throughout. In the vertical section of the riser, the dead flow zone in the corner together with crystal accumulation resulted in a layer that obstructed about half of the opening.

The RSM test showed that it is possible for small parts of accumulated layers to be removed during normal pouring. An accident with two large pouring events, with most of the glass removed from the melter in a relatively short time period, showed that even complete removal of the layer is possible if more vigorous convection currents in conjunction with heating of the riser are provided during pouring.

Electrical conductivity probe testing showed that this method can be used to monitor accumulation of spinel crystals in the riser section of the melter. However, more tests are needed to develop this method to the stage of commercial use.

The long-term RSM test also showed that more attention should be paid to the off-gas system. Maintenance was required on a regular basis to prevent clogging of the off-gas system.

8.0 References

Edwards M, J Matyáš, and J Crum. 2017. “Real-time monitoring of crystal accumulation in the high-level waste glass melters using an electrical conductivity method” *International Journal of Applied Glass Science* 9:42–51. DOI: 10.1111/ijag.12275.

Goles RW and AJ Schmidt. 1992. *Evaluation of Liquid-Fed Ceramic Melter Off-Gas System Technologies for the Hanford Waste Vitrification Plant*. PNL-8109, Pacific Northwest Laboratory, Richland, Washington. Accessed April 6, 2018, at https://www.osti.gov/servlets/purl/10156745.

Matyáš J, GJ Sevigny, MJ Schweiger, and AA Kruger. 2015. “Research-Scale Melter: An Experimental Platform for Evaluating Crystal Accumulation in High-Level Waste Glasses.” Chapter 5 in *Advances in Materials Science for Environmental and Energy Technologies IV: Ceramic Transactions*, Volume 253, 49–59. DOI: 10.1002/9781119190042.ch5.

Matyáš J, JD Vienna, A Kimura, M Schaible, and RM Tate. 2010. “Development of crystal-tolerant waste glasses.” *Ceramic Transactions* 222:41–51.

Matyáš J, V Gervasio, SE Sannoh, and AA Kruger. 2017. “Predictive modeling of crystal accumulation in high-level waste glass melters processing radioactive waste.” *Journal of Nuclear Materials* 495:322–331. DOI: 10.1016/j.jnucmat.2017.08.034.

Distribution

No. of Copies	
2	U.S. Department of Energy Office of River Protection AA Kruger T Fletcher J Grindstaff J Peshong
#	Savannah River National Laboratory KM Fox

No. of Copies	
#	**Local Distribution** Pacific Northwest National Laboratory CP Bonham SK Cooley WC Eaton V Gervasio T Jin JB Lang JM Mayer BP McCarthy GF Piepel RL Russell MJ Schweiger BA Stanfill P Hrma JD Vienna Information Release (PDF)

Pacific Northwest National Laboratory

902 Battelle Boulevard
P.O. Box 999
Richland, WA 99352
1-888-375-PNNL (7665)

www.pnnl.gov

BATTELLE

U.S. DEPARTMENT OF ENERGY